

Topological Superconductor-Luttinger Liquid Junctions

Ian Affleck¹ and Domenico Giuliano²

¹ Department of Physics and Astronomy, University of British Columbia, Vancouver, B.C., Canada, V6T 1Z1

² Dipartimento di Fisica, Università della Calabria Arcavacata di Rende I-87036, Cosenza, Italy and I.N.F.N., Gruppo collegato di Cosenza, Arcavacata di Rende I-87036, Cosenza, Italy

E-mail:

¹ iaffleck@phas.ubc.ca

² domenico.giuliano@fis.unical.it

Abstract. Experimental evidence was recently obtained for topological superconductivity in spin-orbit coupled nano wires in a magnetic field, proximate to an s-wave superconductor. When only part of the wire contacts the superconductor, a localized Majorana mode exists at the junction between superconducting and normal parts of the nanowire. We consider here the case of a T-junction between the superconductor and two normal nanowires and also the case of a single wire with two (or more) partially filled bands in the normal part. We find that coupling this 2-channel Luttinger liquid to the single Majorana mode at the junction produces frustration, leading to a critical point separating phases with perfect Andreev scattering in one channel and perfect normal scattering in the other.

PACS numbers: 73.21.Hb, 71.10.Pm, 73.63.Nm

1. Introduction and Conclusions

The existence of Majorana modes in various topological phases has attracted great theoretical and experimental interest due to possible applications to quantum computing. Recently, experimental evidence for such a Majorana mode was obtained in indium antimonide quantum wires, where only part of the wire was proximate to an s-wave superconductor [1], following theoretical proposals in [2, 3]. A Majorana mode is expected to be localized at the (SN) junction between superconducting and normal parts of the wire. [See figure (1).] Due to the strong spin-orbit coupling, ideally, the quantum wire might have only one active channel in the normal region. Depending on the applied field and other details, two or more channels might instead be active. Many theoretical papers have appeared recently on this and related topics, including [4, 5, 6, 7, 8, 9, 10, 11, 12]. The inspiration for our work was the low energy theoretical approach, in both one and two channel cases, developed in [13], using Luttinger liquid (LL) theory and methods introduced in [14] to treat LL SN junctions. Due to its energy gap, all the electronic degrees of freedom in the superconducting part of the wire may be integrated out, except for the Majorana mode at the junction. In the single channel case, it was found that the system renormalizes, at low energies, to a fixed point characterized by perfect Andreev reflection, leading to an enhanced conductance through the junction. The 2-channel case was also discussed in [13], *but only in the simplified limit where the Majorana mode couples to just 1 of the channels*. It was found that the low energy fixed point has perfect Andreev reflection in the channel coupling to the Majorana mode and perfect normal reflection in the other channel.

Here we extend this analysis to the case where both channels couple to the Majorana mode. The physical situation could correspond to a T-junction between a topological superconductor and 2 single-channel quantum wires, or to a single wire containing two active channels in its normal part. [See Fig. (1).] We find that coupling a single Majorana mode to a two-channel Luttinger liquid leads to an unusual type of frustration. Assuming that the couplings, t_1 and t_2 of the two channels to the Majorana mode are unequal, we find that the larger coupling grows under renormalization and the smaller one shrinks, so that, at low energies, there is perfect Andreev reflection in one channel and perfect normal reflection in the other. This means that the Majorana mode acts as a switch at the T-junction. Even a slight imbalance in tunnel couplings of the two normal wires to the superconductor leads to all the current flowing to the more strongly coupled wire, at low energies. This feature might be of use for implementing gate operations in a proposed [15] quantum computer built from T-junctions. By tuning the tunnel couplings at the junction so $t_1 = t_2$, a critical point can be reached which exhibits non-trivial conductances to both channels and associated unusual scaling exponents. The universal conductance and other critical properties vary continuously with the Luttinger parameters of the 2-channel Luttinger liquid. We are able to calculate these universal numbers in a certain range of Luttinger parameters using “ ϵ -expansion” techniques. We find that this critical behaviour is quite robust, surviving when the 2 Luttinger liquids

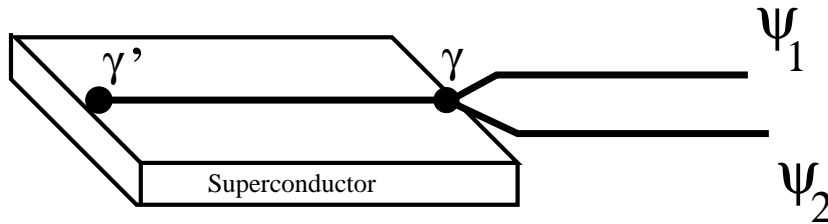


Figure 1. Sketch of the SN junction with a topological superconductor, characterized by the localized Majorana modes γ, γ' at its boundaries, interfaced to two interacting electronic normal channels: these may either be regarded as two active channels within the same wire, or as two different quantum wires interfaced to the topological superconductor.

have different velocities and Luttinger parameters and when they are coupled together in a single quantum wire. Only a single parameter needs to be tuned at the junction to reach the critical point. Similar behaviour occurs for >2 channels. Analogous universal properties are expected to appear, for instance, in the equilibrium Josephson current flowing across the normal region contacted with two topological superconductors at fixed phase difference [16] which, in the low temperature long junction limit, has been shown to depend only on reflection amplitudes at the Fermi level [17].

In Sec. II we analyze the phase diagram of the 2-channel model. Sec. III studies its conductance. In Sec. IV we discuss the generalization to more than 2 channels. Appendix A develops bosonization for 2 coupled channels with different velocities. Appendix B derives the renormalization group equations in the ϵ expansion. Appendix C presents a mapping of the 2-channel Hamiltonian onto an xxz spin chain model containing unusual impurity couplings. Appendix D analyzes the stable fixed point with perfect Andreev scattering in one channel and perfect normal scattering in the other. Appendix E argues for the stability of the non-trivial critical point for general Luttinger parameters. Appendix F considers a single channel uniform wire, coupled to the topological superconductor far from its endpoints, confirming the proposed phase diagram. Appendix G calculates the impurity entropy at the various fixed points.

2. The topological superconductor- 2-channel Luttinger liquid junction

After integrating out the gapped excitations in the superconductor, we are left with a low energy theory describing 2 channels of interacting Dirac fermions coupled to a boundary Majorana mode. The left and right moving Dirac fermions contain the wave-vector components near $\pm k_{Fj}$, the Fermi points, for each channel:

$$\psi_j(x) \approx \exp[ik_{Fj}x]\psi_{Rj}(x) + \exp[-ik_{Fj}x]\psi_{Lj}(x). \quad (1)$$

We write the Hamiltonian:

$$H = H_0 + H_{\text{int}} + H_b. \quad (2)$$

Here H_0 is the Hamiltonian of 2 channels of non-interacting electrons:

$$H_0 \equiv \sum_{j=1}^2 i v_{Fj} \int_0^\infty dx [\psi_{Rj}^\dagger \partial_x \psi_{Rj} - \psi_{Lj}^\dagger \partial_x \psi_{Lj}], \quad (3)$$

and $\psi_{L/R,j}(x)$ annihilates left/right moving electrons in channel $j = 1, 2$. We impose “open boundary conditions” at $x = 0$:

$$\psi_{Rj}(0) = \psi_{Lj}(0) \quad (4)$$

corresponding to disconnected channels before turning on the coupling to the superconductor. v_{Fj} are the Fermi velocities in the two channels. The bulk interactions in general consist of intra-channel and inter-channel terms:

$$H_{\text{int}} = H_{\text{intra}} + H_{\text{inter}}. \quad (5)$$

The most important intra-channel interaction is:

$$H_{\text{intra}} = \sum_j V_j \int_0^\infty dx (: \psi_{Rj}^\dagger \psi_{Rj} : + : \psi_{Lj}^\dagger \psi_{Lj} :)^2. \quad (6)$$

(The $: \dots :$ denote normal ordering.) We assume Umklapp processes can be ignored, true below a critical interaction strength even for commensurate electron densities. The interaction in Eq. (6) changes the Luttinger parameter away from its non-interacting value. Other interactions only change the Fermi velocity or have no effect on the low energy theory. In the case of a T-junction of single channel nano wires, the only important bulk interaction is H_{intra} . In the case of a 2-channel wire, we assume that the bulk interactions conserve the number of electrons in each channel. We also assume $k_{F1} \neq k_{F2}$, likely to be true in a spin-orbit coupled quantum wire in a magnetic field. The most important inter-channel interaction is then:

$$H_{\text{inter}} = U \int_0^\infty dx (: \psi_{L1}^\dagger \psi_{L1} : + : \psi_{R1}^\dagger \psi_{R1} :)(: \psi_{L2}^\dagger \psi_{L2} : + : \psi_{R2}^\dagger \psi_{R2} :). \quad (7)$$

The term $\psi_{L1}^\dagger(x) \psi_{R1}(x) \psi_{L2}^\dagger(x) \psi_{R2}(x)$ comes with an oscillating factor $\exp[2i(k_{F1} - k_{F2})x]$ and can be ignored at low energies. [In the case $k_{F1} = k_{F2}$, this term must be taken into account and could produce a gap.] U mixes the 2 Luttinger liquids. Note that, in the special case $v_{F1} = v_{F2}$, $U/2 = V_1 = V_2$ the model has $SU(2)$ symmetry and it would be natural to interpret 1 and 2 as spin indices. This symmetry is unlikely to occur in a spin-orbit coupled system in a magnetic field. However, it provides a useful consistency check on some of our results, so we will occasionally consider it. Finally, the most important boundary interaction is with the localized Majorana mode, γ , of the topological superconductor:

$$H_b = \gamma \sum_j t_j [\psi_j(0) - \psi_j^\dagger(0)]. \quad (8)$$

Here $\psi_j(0) \equiv \psi_{Lj}(0) = \psi_{Rj}(0)$. By redefining the phases of ψ_j , we will also choose the t_j real and non-negative, $t_j \geq 0$. Most of the new results obtained in this paper arise from considering the general case where t_1 and t_2 are both non-zero. These single electron tunnelling terms from the Luttinger liquid to the superconductor are generally strongly

relevant and determine the low energy physics. In addition, we could add various other boundary interactions, quadratic in $\psi_j(0)$ and $\psi_j^\dagger(0)$, which are generally irrelevant and were discussed in [13].

To study the low energy physics we bosonize the Luttinger liquid. In order to take account of the fermion anti-commutation relations, it is very convenient to introduce Klein factors, Γ_i . The usefulness of bosonization Klein factors for studying related Majorana mode models was pointed out in [18]. Thus we write:

$$\psi_{L/R,j}(x) \propto \Gamma_j \exp\{i\sqrt{\pi}[\phi_j(x) \pm \theta_j(x)]\} \quad (9)$$

with:

$$\{\Gamma_i, \Gamma_j\} = 2\delta_{ij}, \quad \{\Gamma_i, \gamma\} = 0, \quad \gamma^2 = 1. \quad (10)$$

In the T-junction case, with $H_{\text{inter}} = 0$, the bulk Hamiltonian is diagonal in the ϕ_j, θ_j bosons:

$$H_0 + H_{\text{intra}} = \frac{1}{2} \sum_j u_j \int_0^\infty dx \left[K_j \left(\frac{\partial \phi_j}{\partial x} \right)^2 + K_j^{-1} \left(\frac{\partial \theta_j}{\partial x} \right)^2 \right]. \quad (11)$$

Here K_j and u_j are the Luttinger parameters and velocities for the two branches of the T-junction, depending on V_j . (Our Luttinger parameter K corresponds to g in the notation of [13].) In the non-interacting case, $V_j = 0$, $K_j = 1$. When inter-channel interactions, U are included, we can conveniently write ϕ_j in terms of bosons ϕ_ρ, ϕ_σ which diagonalize the bulk Hamiltonian:

$$\begin{pmatrix} \phi_1 \\ \phi_2 \end{pmatrix} = \begin{pmatrix} r^{-1} \cos \alpha & r^{-1} \sin \alpha \\ -r \sin \alpha & r \cos \alpha \end{pmatrix} \begin{pmatrix} \phi_\sigma \\ \phi_\rho \end{pmatrix},$$

$$\begin{pmatrix} \theta_1 \\ \theta_2 \end{pmatrix} = \begin{pmatrix} r \cos \alpha & r \sin \alpha \\ -r^{-1} \sin \alpha & r^{-1} \cos \alpha \end{pmatrix} \begin{pmatrix} \theta_\sigma \\ \theta_\rho \end{pmatrix}. \quad (12)$$

The parameters r and α are a measure the asymmetry between the two channels. In the symmetric case, $v_{F1} = v_{F2}$, $V_1 = V_2$, $\alpha = \pi/4$ and $r = 1$. See Appendix A for a derivation of these results. ([13] only considered the symmetric case, $\alpha = \pi/4$, $r = 1$.) The bulk Hamiltonian becomes:

$$H_0 = \sum_{\lambda=\rho,\sigma} \frac{u_\lambda}{2} \int_0^\infty dx \left[K_\lambda \left(\frac{\partial \phi_\lambda}{\partial x} \right)^2 + K_\lambda^{-1} \left(\frac{\partial \theta_\lambda}{\partial x} \right)^2 \right]. \quad (13)$$

The subscripts ρ and σ refer to charge and spin in the Luttinger liquid literature but that interpretation is general not appropriate in this case. A T-junction with inequivalent wires can be regarded as the special case $\alpha = 0$, with $K_1 = K_\sigma r^2$ and $K_2 = K_\rho/r^2$. In the non-interacting limit, $K_\rho/r^2 = K_\sigma r^2 = 1$. In the SU(2) symmetric case, $V_1 = V_2 = U/2$, $v_{F1} = v_{F2}$, $r = 1$, $\alpha = \pi/4$ and K_σ remains fixed at the value 1. The normal reflection boundary condition of Eq. (4) corresponds to:

$$\theta_j(0) = \text{constant} \quad (14)$$

so the bosonized boundary Hamiltonian is:

$$H_b = i\gamma \sum_j t_j \tau_0^{-1+d_j} \Gamma_j \{ \exp[i\sqrt{\pi}\phi_j(0)] + \exp[-i\sqrt{\pi}\phi_j(0)] \}, \quad (15)$$

with τ_0^{-1} being a high-energy cutoff. For convenience, we redefine the normalization of the dimensionless tunnelling parameters, t_j , so that the boundary operators $\exp[\pm i\sqrt{\pi}\phi_j(\tau)]$ are unit normalized:

$$\mathbf{T} < \exp[i\sqrt{\pi}\phi_j(\tau)] \exp[-i\sqrt{\pi}\phi_j(0)] > = \frac{1}{|\tau|^{2d_j}}. \quad (16)$$

Here \mathbf{T} denotes (imaginary) time-ordering and $\phi_j(\tau) \equiv \phi_j(\tau, x = 0)$. Taking into account the boundary conditions of Eq. (14), in the T-junction case:

$$2d_j = \frac{1}{K_j}. \quad (17)$$

With inter-channel interactions:

$$\begin{aligned} 2d_1 &= r^{-2} \left(\frac{\cos^2 \alpha}{K_\sigma} + \frac{\sin^2 \alpha}{K_\rho} \right) \\ 2d_2 &= r^2 \left(\frac{\sin^2 \alpha}{K_\sigma} + \frac{\cos^2 \alpha}{K_\rho} \right). \end{aligned} \quad (18)$$

The d_i are the renormalization group scaling dimensions of the boundary interactions, implying the scaling equations:

$$-\frac{dt_i}{d \ln D} = (1 - d_i)t_i + \dots, \quad (19)$$

with D being a running high energy cut-off. For non-interacting electrons, $d_i = 1/2$ so that the couplings to the Majorana mode are strongly relevant. We expect the d_i to increase as repulsive interactions are turned on, but the t_i remain relevant ($d_i < 1$) up to quite strong repulsive interactions.

The low temperature conductance and other low energy properties of the SN junction are determined by the infrared stable fixed point of these renormalization group (RG) equations. In the case where $t_2 = 0$ (or equivalently $t_1 = 0$) it was argued in [13] that t_1 renormalizes to large values and t_2 remains at zero. This fixed point corresponds to a conformally invariant boundary condition:

$$\begin{aligned} \phi_1(0) &= 0 \quad \text{or} \quad \sqrt{\pi} \\ \theta_2(0) &= 0. \end{aligned} \quad (20)$$

The two possible boundary conditions [13] on ϕ_1 in Eq. (20) correspond to eigenstates of $i\gamma\Gamma_1$ with eigenvalue -1 and $+1$ respectively. To see that such eigenstates exist, note that we may combine γ and Γ_1 into a Dirac operator localized at the junction:

$$\psi_0 \equiv \frac{\gamma + i\Gamma_1}{2} \quad (21)$$

obeying $\{\psi_0, \psi_0^\dagger\} = 1$. We then have:

$$i\gamma\Gamma_1 = 2(\psi_0^\dagger\psi_0 - 1/2) \quad (22)$$

which clearly has eigenvalues ± 1 . These are ‘‘Schroedinger cat states’’ in which a single electron has equal amplitude to be in the superconductor or in the nanowire (in channel 1). This can be seen by observing that there is actually a second Majorana mode,

γ' localized at the opposite end of the superconductor, far from the SN junction, as sketched in Fig. 1. We may construct a different Dirac zero mode operator

$$\psi_S \equiv \frac{\gamma + i\gamma'}{2}. \quad (23)$$

This annihilates an electron which is located entirely inside the superconductor but is highly delocalized, with equal amplitudes at both ends. Denoting the corresponding states as $|0S\rangle$ and $|1S\rangle$, we see that that $\gamma|0S\rangle = |1S\rangle$. Thus the eigenstates of $i\gamma\Gamma_1$ are linear superpositions of $|0S\rangle$ and $|1S\rangle$.

As shown in [14, 13], the boundary condition of Eq. (20) corresponds to perfect Andreev scattering at the SN junction in channel 1 and perfect normal scattering in channel 2 and the corresponding boundary conditions are labelled $A \otimes N$.

The main question we wish to address in this paper is the nature of the ground state when t_1 and t_2 are both non-zero. This is readily addressed for the non-interacting model, $V_i = U = 0$. Then we can make a change of basis:

$$\begin{aligned} \tilde{\psi}_1 &= \frac{t_1\psi_1 + t_2\psi_2}{\sqrt{t_1^2 + t_2^2}} \\ \tilde{\psi}_2 &= \frac{-t_2\psi_1 + t_1\psi_2}{\sqrt{t_1^2 + t_2^2}}. \end{aligned} \quad (24)$$

so that

$$H_b \rightarrow \gamma\sqrt{t_1^2 + t_2^2}[\tilde{\psi}_1(0) - \tilde{\psi}_1^\dagger(0)]. \quad (25)$$

Clearly the ground state corresponds to perfect Andreev scattering in channel $\tilde{1}$ and perfect normal scattering in channel $\tilde{2}$. An electron from channel $\tilde{1}$ is in an entangled state with the superconductor. We refer to these as rotated $A \otimes N$ boundary conditions. It is basically the $SU(2)$ symmetry of the free electron model which allows us to form this superposition. We might worry that unequal Fermi velocities in the two non-interacting channels destroy this $SU(2)$ symmetry. However, since we only need to make the unitary transformation at the boundary, and the system is non-interacting, we can rescale the x -coordinate differently for the two channels and again make this transformation. In general, such a transformation cannot be conveniently made in the interacting case. An exception occurs when $v_{F1} = v_{F2}$ and $V_1 = V_2 = U/2$ so that the model has $SU(2)$ symmetry. In this case we can always make the transformation of Eq. (24) and obtain a rotated $A \otimes N$ boundary condition. Formally, we may make the $SU(2)$ transformation first, and then bosonize. The RG flow diagram in this case corresponds to Fig. (2).

It is important to note that the rotated $A \otimes N$ boundary condition is very different from an $A \otimes A$ boundary condition despite the fact that the tunnelling amplitudes, t_i , to both channels, renormalized to large values. In an $A \otimes N$ state, the Majorana mode is strongly entangled with *one linear combination* of fermion fields and the orthogonal linear combination decouples. This corresponds to a stable fixed point of the system as we show later in this section and in Appendix D. On the other hand, in an $A \otimes A$ state, the Majorana mode is strongly entangled with *both* fermion fields. This turns out to be an unstable fixed point, as we will show in Appendix E.

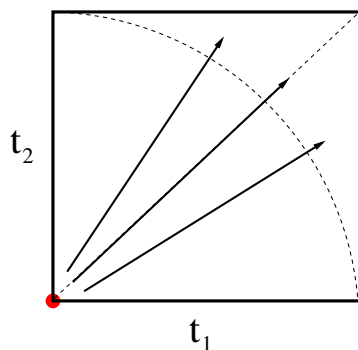


Figure 2. Plot of the flow of the effective tunnelling amplitudes with decreasing energy scale in the $SU(2)$ symmetric case.

It is far from obvious at this stage what the low energy behavior is for the general non- $SU(2)$ invariant interacting case, with $t_1, t_2 > 0$. To gain some insight into this question, we calculate the terms of next order in t_i in the β -functions of Eq. (19). This calculation is of interest primarily in the case where $0 < 1 - d_i \ll 1$, since then the β -functions may have a zero (corresponding to a renormalization group fixed point) at small t_i where stopping the expansion at next order can be justified. It is then convenient to define:

$$\epsilon_i \equiv 1 - d_i. \quad (26)$$

To calculate the next order terms in the β -functions we thus set $\epsilon_1 = \epsilon_2 = 0$, corresponding to marginal interactions. Thus the four parameters labelling the bulk interactions are reduced to 2 independent parameters by the conditions, following from Eq. (18):

$$r^{-2} \left(\frac{\cos^2 \alpha}{K_\sigma} + \frac{\sin^2 \alpha}{K_\rho} \right) = r^2 \left(\frac{\cos^2 \alpha}{K_\rho} + \frac{\sin^2 \alpha}{K_\sigma} \right) = 2. \quad (27)$$

The detailed calculation of these β -functions is given in Appendix B. The quadratic terms can easily be seen to vanish and the cubic terms are given in terms of a single function of the interactions parameters,

$$\nu \equiv \frac{\sin 2\alpha}{2} \left(\frac{1}{K_\rho} - \frac{1}{K_\sigma} \right). \quad (28)$$

These have the form:

$$\begin{aligned} \frac{dt_1}{dl} &= \epsilon_1 t_1 - \mathcal{F}(\nu) t_1 (t_2)^2 \\ \frac{dt_2}{dl} &= \epsilon_2 t_2 - \mathcal{F}(\nu) t_2 (t_1)^2. \end{aligned} \quad (29)$$

Here $l \equiv -\ln D$. The function $\mathcal{F}(\nu)$ is given as a 1-dimensional integral in Eq. (B.41) and plotted in Fig. (B1). It is monotone decreasing, passing through 0 at $\nu = 1$. This latter value provides an important check on our calculations. The bulk theory has $SU(2)$ invariant when $r = 1$, $\alpha = \pi/4$ and $K_\sigma = 1$. The condition Eq. (27) for the interactions be marginal then determines $K_\rho = 1/3$ and hence, from Eq. (28), $\nu = 1$. Thus, $\mathcal{F} = 0$

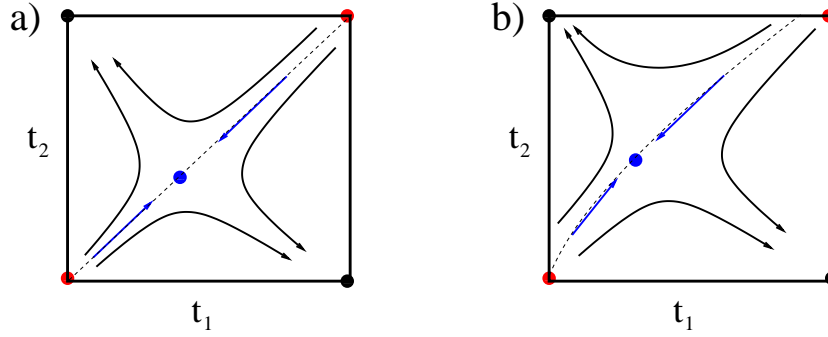


Figure 3. Flow of the effective tunnelling amplitudes with decreasing energy scale. a) The symmetric case $\epsilon_1 = \epsilon_2$. The red dots represent the completely unstable $N \otimes N$ and $A \otimes A$ fixed points, the blue dot represents the non-trivial critical point and the black dots represent the stable $A \otimes N$ and $N \otimes A$ critical points. The unstable $A \otimes A$ fixed is discussed in Appendix E. b) An example of the general case.

for the $SU(2)$ invariant model. This is consistent with our observation that the RG flows are along rays in the $t_1 - t_2$ plane, flowing towards strong coupling in that case, as shown in Fig. (2). Note that the T-junction corresponds to $\alpha = 0$ and then Eq. (27) gives $K_\rho = K_\sigma = 1/2$ and thus $\nu = 0$ and $\mathcal{F} = 4$.

In general, for $\nu < 1$, where $\mathcal{F}(\nu) > 0$, the RG equations have a fixed point at:

$$\begin{aligned} t_{1c} &= \sqrt{\frac{\epsilon_2}{\mathcal{F}(\nu)}} \\ t_{2c} &= \sqrt{\frac{\epsilon_1}{\mathcal{F}(\nu)}}. \end{aligned} \quad (30)$$

Taking $\epsilon_i \rightarrow 0$ for any fixed ν , this fixed point occurs at weak coupling where higher order terms in the β -function can be ignored. The corresponding RG flow diagram is sketched in Fig. (3). This nontrivial critical point (NTCP) has one unstable direction, and one stable direction in the $t_1 - t_2$ plane. In the symmetric case $\epsilon_1 = \epsilon_2$, the unstable direction corresponds to making the t_i 's unequal:

$$\begin{aligned} t_1 &= t_c + \delta t \\ t_2 &= t_c - \delta t. \end{aligned} \quad (31)$$

Eqs. (29) then imply:

$$\frac{d(\delta t)}{dl} = 2\epsilon \delta t + \dots \quad (32)$$

On the other hand, the NTCP is stable along the symmetry line where:

$$\begin{aligned} t_1 &= t_c + \delta t \\ t_2 &= t_c + \delta t, \end{aligned} \quad (33)$$

and thus

$$\frac{d(\delta t)}{dl} = -2\epsilon \delta t + \dots \quad (34)$$

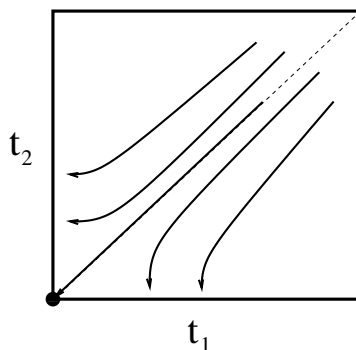


Figure 4. Flow of the effective tunnelling amplitudes with decreasing energy scale, for the case of marginal boundary couplings, $\epsilon_i = 0$.

Note that when the ϵ_i are strictly zero, the RG equations, Eq. (29) imply lines of stable fixed points along the t_1 and t_2 axes as shown in Fig. (4). This type of flow diagram was discussed in [19, 20] as a model for a 2-level system interacting with 2 independent heat baths, where it corresponded to “frustration of decoherence”. In Appendix C, we show that a special case with $\epsilon_i = 0$ corresponds to an unusual anisotropic version of the 2-channel Kondo model. The model with decoupled equivalent chains, $U = 0$, $v_{F1} = v_{F2}$, $V_1 = V_2$ arbitrary, turns out to be identical to a formulation of the dissipative Hofstadter model [22], studied in [21]. This can be seen from the spin chain representation of our model, introduced in Appendix C; precisely the same model was studied in [21], in this special case. The β functions of Eq. (29) were already obtained, and their fixed point analyzed, for this case. This model and β -function are also closely related to ones studied earlier in the context of the dissipative Hofstadter model and of the Bose-Fermi Kondo model [23]. For $\epsilon_1 = \epsilon_2 = \nu = 0$ the β function in Eq.(29) also describes the “paperclip model” at topological angle $\vartheta = \pi$ studied in [24]. However for the general case, with $V_1 \neq V_2$, $U \neq 0$ and arbitrary α , these NTCP’s are *not* equivalent to any other previously discovered ones that we are aware of. Note that, moving away from the NTCP along the unstable direction, the flow is towards $(t_1, t_2) = (\infty, 0)$ or $(0, \infty)$ corresponding to $A \otimes N$ or $N \otimes A$ fixed points. These fixed points are stable [13] and thus it is plausible that the RG flow goes to them in all cases.

So far, we have only established this phase diagram for small ϵ_i . However, we expect that it remains qualitatively similar for a finite range of bulk interaction parameters (K_ρ , K_σ , r and α). Arguments are presented for this in a series of Appendices. In Appendix D we show that the $A \otimes N$ and $N \otimes A$ fixed points are stable over a large range of bulk interaction parameters. In Appendix E, we give arguments for the existence of the NTCP. In particular, we discuss the unstable $A \otimes A$ fixed point, shown in Fig. (3) at $t_1 = t_2 = \infty$. We also mention a possible alternative to the phase diagram of Fig. (3) which might conceivably occur for a range of Luttinger parameters but requires additional nontrivial critical points. In Appendix F we consider a model of a uniform single channel quantum wire coupled far from its ends to the topological superconductor. For $2 - \sqrt{3} \approx .268 < K < 1$, we find that the RG flow is again to $A \otimes N$ or $N \otimes A$

or else to the NTCP if an appropriate symmetry is respected. This strongly supports the universality of our proposed phase diagram, Fig. (3). In Appendix G we calculate the universal impurity entropy at the various fixed points and show that our proposed phase diagram is consistent with the g -theorem [33, 34, 35].

The phase diagram of Fig. (3) is perhaps especially interesting in the T -junction case. If such a junction could be tuned close to the critical point by adjusting the t_i 's with gate voltages, its behavior would become extremely sensitive to small changes in these gates, which would drive it away from the NTCP to $A \otimes N$ or $N \otimes A$. As discussed in the next section, this behaviour could be measured from the low energy conductance through the junction. A slight detuning of the tunnelling amplitudes would produce zero conductance to one wire and perfect Andreev conductance to the other, at low energies.

3. Conductance

Conductance measurements might provide experimental observation of the NTCP found in the previous section. Labelling the 3 arms of the T -junction by 1 and 2 for the two Luttinger liquid channels and 0 for the superconducting quantum wire, we consider voltages V_k applied to channel k and currents I_j flowing in arm j , towards the junction. The linear conductance tensor, G_{jk} is then defined by:

$$I_j = \sum_{k=0}^2 G_{jk} V_k. \quad (35)$$

Conservation of charge and the condition that no current flows when all voltages are equal imply:

$$\sum_j G_{jk} = 0 = \sum_k G_{jk} = 0. \quad (36)$$

Let us first consider the case where the tunnelling amplitudes have been fine-tuned so that the system flows to the NTCP at low energies. Within our ϵ -expansion, we may calculate the conductance at zero temperature, zero frequency and zero source-drain voltage, V , in second order perturbation theory in the tunnelling amplitudes, t_i , using their fixed point values t_{ic} . A closely related calculation is done in [25], Appendix A [26]. In that paper the bosonized tunnelling term was written $H_b = t \cos \sqrt{\pi} \phi$. Apart from a factor of 2 in the definition of t , the main difference in our case is the presence of the Majorana mode and Klein factor $\gamma \Gamma_i$. The perturbative calculation just requires calculating the 2-point Green's function of the tunnelling operator:

$$\mathcal{T} < \gamma(\tau) \Gamma_j(\tau) e^{i\sqrt{\pi}\phi_j(\tau)} \gamma(0) \Gamma_j(0) e^{-i\sqrt{\pi}\phi_j(0)} > . \quad (37)$$

Using:

$$\mathcal{T} < \gamma(\tau) \gamma(0) > = \mathcal{T} < \Gamma_j(\tau) \Gamma_j(0) > = \epsilon(\tau), \quad (38)$$

the anti-symmetric step function, we see that the product of Majorana mode and Klein factor Green's function is unity leading to

$$\mathcal{T} < \gamma(\tau) \Gamma_j(\tau) e^{i\sqrt{\pi}\phi_j(\tau)} \gamma(0) \Gamma_j(0) e^{-i\sqrt{\pi}\phi_j(0)} > = -\frac{1}{\tau^2}. \quad (39)$$

Here we have set $\epsilon_j = 0$, valid to lowest order. This corresponds to $n^2 g = 1$, $\lambda = 2$, in the notation of [25], Appendix A. Noting that the functions of [25] Appendix A take values $f_1(2) = f_3(2) = \pi$, the current flowing to channel j in response to a voltage difference V_j is $I = G_{jc} V_j$, with:

$$G_{jc} = (e^2/h)(\pi t_{jc})^2. \quad (40)$$

From Eq. (30) this gives:

$$\begin{aligned} G_{1c} &= \frac{e^2 \pi^2}{h} \frac{\epsilon_2}{\mathcal{F}(\nu)} \\ G_{2c} &= \frac{e^2 \pi^2}{h} \frac{\epsilon_1}{\mathcal{F}(\nu)}. \end{aligned} \quad (41)$$

It can readily be seen that, to $O(\epsilon_i)$, no current flows from channel 1 to channel 2 in linear response to a voltage difference. Following the method of [25] and [27] for the T -junction case, this holds because the perturbative expansion of the partition function does not contain a term of $O(t_1 t_2)$. It then follows, using Eq. (36) that the full conductance tensor at the non-trivial critical point, to $O(\epsilon_i)$ is:

$$G = \begin{pmatrix} G_{1c} + G_{2c} & -G_{1c} & -G_{2c} \\ -G_{1c} & G_{1c} & 0 \\ -G_{2c} & 0 & G_{2c} \end{pmatrix}. \quad (42)$$

So far we have failed to take into account the fact that the Luttinger liquid quantum wire (or wires) will be of finite length and may be contacted by Fermi liquid leads far from the SN junction. As discussed in [13], in the case of adiabatic contacts of the interacting quantum wires to Fermi liquid leads, this may be modelled by frequency dependent Luttinger parameters which have the values (K_ρ, K_σ) at higher frequencies but eventually cross over to the free Fermion values (1,1) at low frequencies, of order $\omega_\ell \equiv v_F/\ell$ where ℓ is the length of the wires. We might then expect the results of Eq. (41) to hold at frequencies above ω_ℓ but the result for a Majorana SN junction to free fermion channels to hold below ω_ℓ . This would correspond to the rotated $A \otimes N$ fixed point discussed above with total conductance, summed over both channels, of $G_{11} + G_{22} = 2e^2/h$.

At frequencies above ω_ℓ , the conductance should exhibit a universal scaling behaviour as the NTCP is approached. For small ϵ , and choosing, for simplicity, $\epsilon_1 = \epsilon_2 = \epsilon$

$$G_{jj}(\omega) \rightarrow G_{jc} \left\{ 1 - \left(\frac{\omega}{\omega^*} \right)^{2\epsilon} \right\}, \quad (43)$$

where ω^* is a cross-over energy scale. [This is assuming weak bare tunnelling, t . For stronger tunnelling, larger than the critical value, the sign would be positive for the

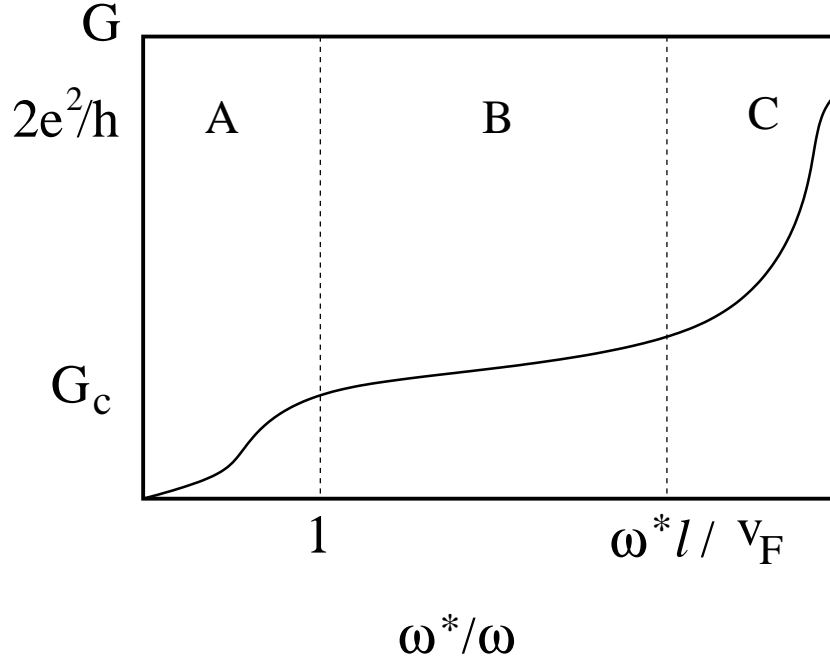


Figure 5. Sketch of the conductance G as a function of ω^*/ω across the NTCP for a junction made with wires of finite length ℓ . For $\omega^*/\omega \ll 1$, the conductance gets small and eventually goes to 0 for $\omega^*/\omega \rightarrow 0$, which is the appropriate behavior in the neighborhood of the $N \otimes N$ -fixed point (region A of the plot). For $1 \leq \omega^*/\omega \leq \omega^*\ell/v_F$, the conductance takes a value of the order of G_c , showing that, in this region, the transport properties of the junction are controlled by the NTCP (region B of the plot). Finally, for $\omega^*/\omega > \omega^*\ell/v_F$ the conductance flows towards $2e^2/h$, corresponding to the onset of the rotated $A \otimes N$ -fixed point, due to coupling of wires of finite length ℓ to Fermi liquid reservoirs.

second term in Eq. (43).] Using our exact solution for the RG flow at small ϵ , in the limit of weak bare tunnelling, the full crossover is given by:

$$G_{jj} = \frac{e^2\pi^2}{h} \frac{\epsilon}{\mathcal{F}(\nu)} \frac{1}{1 + (\omega/\omega^*)^{2\epsilon}} \quad (44)$$

approaching zero at ω much greater than the crossover scale, ω^* where the $N \otimes N$ fixed point is approached. This behaviour is sketched in Fig. (5) showing the crossover with increasing frequency between the 3 different fixed points.

If the ratio of tunnelling amplitudes, t_1/t_2 is not perfectly tuned to 1 we expect more complicated crossover behaviour with increasing ω . As ω is raised the system goes from rotated $A \otimes N$ to unrotated $A \otimes N$ to non-trivial to $N \otimes N$ fixed points. Assuming, for simplicity, $\epsilon_1 = \epsilon_2$, and t_1 slightly bigger than t_2 , the flow away from the NTCP is described by:

$$\begin{aligned} G_{11} &= \frac{e^2\pi^2}{h} \frac{\epsilon}{\mathcal{F}(\nu)} [1 + \delta t (\tilde{\omega}^*/\omega)^{2\epsilon}] \\ G_{22} &= \frac{e^2\pi^2}{h} \frac{\epsilon}{\mathcal{F}(\nu)} [1 - \delta t (\tilde{\omega}^*/\omega)^{2\epsilon}] \end{aligned} \quad (45)$$

where $\delta t \equiv t_1 - t_2$ and $\tilde{\omega}^*$ is another crossover scale.

At the $A \otimes N$ fixed point the conductance tensor is given by [13]

$$G = \frac{K_1 2e^2}{h} \begin{pmatrix} 1 & -1 & 0 \\ -1 & 1 & 0 \\ 0 & 0 & 0 \end{pmatrix}. \quad (46)$$

Including adiabatic connections to Fermi liquid leads, the factor of K_1 in Eq. (46) should be set to 1. At low but non-zero temperature the other components of the conductance are non-zero and are controlled by the leading irrelevant operators at the $A \otimes N$ fixed point which can transport electrons between the superconductor and wire 2 or between wire 1 and wire 2. These are given in Eq. (D.7) and (D.8) respectively, leading to:

$$\begin{aligned} G_{02} &\propto T^{4/K_2-2} \\ G_{12} &\propto T^{K_1+1/K_2-2}. \end{aligned} \quad (47)$$

4. More channels

The analysis of Sec. II may be straightforwardly generalized to the case of a single superconducting wire interacting with k normal channels, corresponding, for example, to a T-junction with several channels in each normal branch. The crucial interaction between the single Majorana mode and the normal channels is again given by Eq. (8) with the sum now running over k channels. We may again bosonize, introducing k Klein factors. For a wide range of Luttinger parameters we expect the only stable RG fixed points to correspond to perfect Andreev reflection in one channel and perfect normal reflection in all the rest. This can be confirmed from the RG equations in the case where all tunnelling parameters, t_i , have RG scaling dimensions $d_i = 1 - \epsilon_i$, with $0 < \epsilon_i \ll 1$. Due to the Klein factors, it is easily seen that the RG equations, to cubic order, generally take the form:

$$\frac{dt_i}{dl} = \epsilon_i t_i - t_i \sum_{j \neq i} \mathcal{F}_{ij} t_j^2 \quad (48)$$

where the parameters ϵ_i and \mathcal{F}_{ij} depend on the various intra-channel and inter-channel bulk interactions in the normal wires. Again we see that these equations allow one tunnelling parameter, t_i , to flow to strong coupling while the rest flow to zero, corresponding to the above fixed points. In addition, there will be various less stable non-trivial critical points. Consider, for example, the simplest case with 3 channels, all ϵ_i equal to a common value ϵ and all \mathcal{F}_{ij} having the common value \mathcal{F} . Then Eq. (48) reduces to:

$$\begin{aligned} \frac{dt_1}{dl} &= \epsilon t_1 - \mathcal{F} t_1 [(t_2)^2 + (t_3)^2] \\ \frac{dt_2}{dl} &= \epsilon t_2 - \mathcal{F} t_2 [(t_1)^2 + (t_3)^2] \\ \frac{dt_3}{dl} &= \epsilon t_3 - \mathcal{F} t_3 [(t_1)^2 + (t_2)^2]. \end{aligned} \quad (49)$$

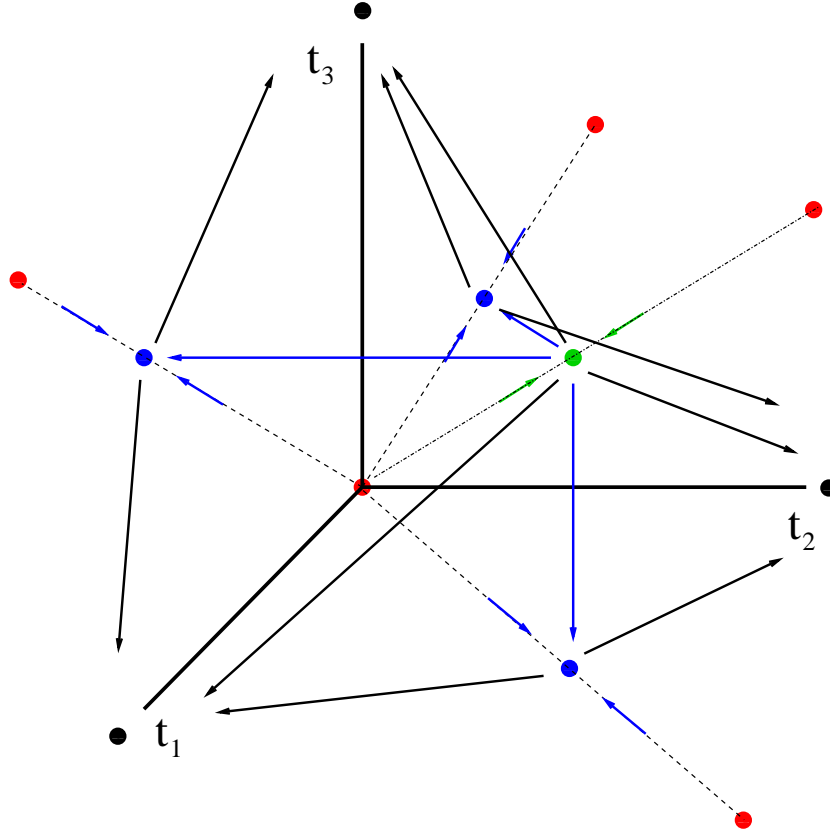


Figure 6. Plot of the flows of the effective tunnelling amplitudes with decreasing energy scale, corresponding to Eq. (49). There is a flow from completely unstable $N \otimes N \otimes N$ and $A \otimes A \otimes A$ critical points to the highly unstable critical point on the main diagonal (green dot) to more stable ones on the 3 planes (blue dots), to totally stable ones at ∞ along the axes (black dots).

Without loss of generality, we may again assume all $t_i \geq 0$. Clearly there is an unstable critical point along the main diagonal at

$$t_1 = t_2 = t_3 = \sqrt{\epsilon/2\mathcal{F}}, \quad (50)$$

In addition, there is an unstable critical point in the t_1 - t_2 plane at

$$t_1 = t_2 = \sqrt{\epsilon/\mathcal{F}}, \quad t_3 = 0, \quad (51)$$

as well as 2 other equivalent critical points in the t_2 - t_3 and t_1 - t_3 planes. The RG flows are sketched in Fig. (6). 2 parameters need to be fine-tuned, $t_1 = t_2 = t_3$, to stabilize the critical point on the main diagonal but only 1 parameter needs to be adjusted, $t_1 = t_2$, to stabilize the critical point in the t_1 - t_2 plane. The only stable fixed points are along the axes at $t_1 = \infty$, $t_2 = t_3 = 0$, etc. A similar hierarchy of non-trivial critical points occurs in the general case. Thus we see that the Majorana mode acts as a switch at low energies in a multi-channel T-junction, or in a junction with an arbitrary number of normal arms. Furthermore we might expect a non-trivial critical point, which can be stabilized by tuning a single tunnelling amplitude, to exist in a multi-channel T-junction.

We would like to thank Hamed Karimi, Yashar Komijani, Eduardo Novais, Zheng Shi and Arturo Tagliacozzo for useful comments about this work; DG would like to thank the Department of Physics and Astronomy of the University of British Columbia for the kind hospitality during the completion of this work. This research was supported by NSERC and CIFAR.

Appendix A. Bosonization of 2 channel model

The most general parity invariant quadratic Hamiltonian is:

$$\mathcal{H} = \frac{1}{2} \sum_j u_j \left[K_j (\partial_x \phi_j)^2 + K_j^{-1} (\partial_x \theta_j)^2 \right] + U_\phi \partial_x \phi_1 \partial_x \phi_2 + U_\theta \partial_x \theta_1 \partial_x \theta_2. \quad (\text{A.1})$$

Of primary interest is the case $U_\phi = 0$, $U_\theta = U/\pi$ corresponding to a pure density-density interaction. This follows from

$$\rho_j(x) \equiv: \psi_{Rj}^\dagger \psi_{Rj} : + : \psi_{Lj}^\dagger \psi_{Lj} := -\frac{1}{\sqrt{\pi}} \partial_x \theta_j. \quad (\text{A.2})$$

The continuum model:

$$\mathcal{H} = \sum_j [i v_{Fj} (\psi_{Rj}^\dagger \partial_x \psi_{Rj} - \psi_{Lj}^\dagger \partial_x \psi_{Lj}) + V_j \rho_j^2] + U \rho_1 \rho_2 \quad (\text{A.3})$$

bosonizes into Eq. (A.1) with:

$$u_j K_j = v_{Fj}, \quad u_j K_j^{-1} = v_{Fj} + V_j/\pi, \quad U_\theta = U/\pi, \quad U_\phi = 0. \quad (\text{A.4})$$

The most general transformation we can make on $\vec{\phi}$ and $\vec{\theta}$ which is canonical, preserving the commutation relations:

$$[\phi_j(x), \theta_k(y)] = -\frac{i}{2} \epsilon(x-y), \quad (\text{A.5})$$

is:

$$\vec{\phi} = M \vec{\phi}', \quad \vec{\theta} = (M^{-1})^T \vec{\theta}' \quad (\text{A.6})$$

for an arbitrary real matrix M . A sufficiently general choice of M to diagonalize the Hamiltonian when $U_\phi = 0$ is:

$$M = \begin{pmatrix} r^{-1} \cos \alpha & r^{-1} \sin \alpha \\ -r \sin \alpha & r \cos \alpha \end{pmatrix}, \quad (M^{-1})^T = \begin{pmatrix} r \cos \alpha & r \sin \alpha \\ -r^{-1} \sin \alpha & r^{-1} \cos \alpha \end{pmatrix} \quad (\text{A.7})$$

for an angle α and a real positive number r . The other two free parameters in M correspond to rescaling ϕ'_j s and θ'_j s, equivalently rescaling the K'_j 's. Requiring the off-diagonal terms in \mathcal{H} to vanish gives:

$$r^4 = \frac{u_1 K_1}{u_2 K_2} \quad (\text{A.8})$$

and

$$\frac{\cos^2 \alpha - \sin^2 \alpha}{\cos \alpha \sin \alpha} = \frac{r^{-2} u_2 K_2^{-1} - r^2 u_1 K_1^{-1}}{U/\pi} \quad (\text{A.9})$$

implying

$$\tan 2\alpha = 2 \frac{\sqrt{u_1 u_2 K_1 K_2} U}{\pi(u_2^2 - u_1^2)}. \quad (\text{A.10})$$

The velocities and Luttinger parameters of the transformed fields are then determined by:

$$u'_1 K'_1 = u_1 K_1 r^{-2} \cos^2 \alpha + u_2 K_2 r^2 \sin^2 \alpha \quad (\text{A.11})$$

$$u'_1 (K'_1)^{-1} = u_1 K_1^{-1} r^2 \cos^2 \alpha + u_2 K_2^{-1} r^{-2} \sin^2 \alpha - 2U \cos \alpha \sin \alpha / \pi \quad (\text{A.12})$$

$$u'_2 K'_2 = u_1 K_1 r^{-2} \sin^2 \alpha + u_2 K_2 r^2 \cos^2 \alpha \quad (\text{A.13})$$

$$u'_2 (K'_2)^{-1} = u_1 K_1^{-1} r^2 \sin^2 \alpha + u_2 K_2^{-1} r^{-2} \cos^2 \alpha + 2U \cos \alpha \sin \alpha / \pi. \quad (\text{A.14})$$

Defining:

$$\tilde{U} \equiv U \sqrt{K_1 K_2} / \pi, \quad (\text{A.15})$$

we have

$$\begin{aligned} \cos 2\alpha &= \frac{u_2^2 - u_1^2}{\sqrt{(u_1^2 - u_2^2)^2 + 4u_1 u_2 \tilde{U}^2}} \\ \sin 2\alpha &= \frac{2\sqrt{u_1 u_2} \tilde{U}}{\sqrt{(u_1^2 - u_2^2)^2 + 4u_1 u_2 \tilde{U}^2}}. \end{aligned} \quad (\text{A.16})$$

Thus:

$$\begin{aligned} u'_{1,2} (K'_{1,2})^{-1} &= \frac{1}{2\sqrt{u_1 u_2 K_1 K_2}} \left[u_1^2 + u_2^2 \mp \sqrt{(u_2^2 - u_1^2)^2 + 4u_1 u_2 \tilde{U}^2} \right] \\ u'_{1,2} K_{1,2} &= \sqrt{u_1 u_2 K_1 K_2}. \end{aligned} \quad (\text{A.17})$$

One application of this transformation is to spinful fermions in a magnetic field. The field makes $k_{F1} \neq k_{F2}$ thus eliminating relevant inter-channel backscattering interactions. It also makes $v_{F1} \neq v_{F2}$, so $u_1 \neq u_2$ giving a 2-component Luttinger liquid exhibiting a generalization of spin-charge separation.

From Eq. (A.17), we see that $u'_1 (K'_1)^{-1}$ vanishes when

$$(u_2^2 + u_1^2)^2 = (u_2^2 - u_1^2)^2 + 4u_1 u_2 \tilde{U}^2, \quad (\text{A.18})$$

implying

$$\tilde{U} = \sqrt{u_1 u_2}. \quad (\text{A.19})$$

Thus the 2 component Luttinger liquid phase is stable for

$$U \leq U_c \equiv \pi \sqrt{u_1 u_2 / (K_1 K_2)}. \quad (\text{A.20})$$

This condition could actually be deduced directly from the Hamiltonian, Eq. (A.1) (for $U_\theta = 0$, $U_\phi = U$.) The terms depending on the θ_j are:

$$H_\theta = \frac{1}{2} (\partial_x \theta_1, \partial_x \theta_2) \begin{pmatrix} u_1 K_1^{-1} & U/\pi \\ U/\pi & u_2 K_2^{-1} \end{pmatrix} \begin{pmatrix} \partial_x \theta_1 \\ \partial_x \theta_2 \end{pmatrix}. \quad (\text{A.21})$$

The condition for this to be positive definite is:

$$\det \begin{pmatrix} u_1 K_1^{-1} & U/\pi \\ U/\pi & u_2 K_2^{-1} \end{pmatrix} = u_1 u_2 / (K_1 K_2) - (U/\pi)^2 > 0. \quad (\text{A.22})$$

If we use the values for u_j , K_j given in Eq. (A.4), obtained from intra-chain interactions, Eq. (A.14) becomes:

$$\begin{aligned} (u_{1',2'})^2 &= \frac{1}{2} \left[v_{F1}(v_{F1} + V_1/\pi) + v_{F2}(v_{F2} + V_2/\pi) \right. \\ &\quad \left. \mp \sqrt{[v_{F2}(v_{F2} + V_2/\pi) - v_{F1}(v_{F1} + V_1/\pi)]^2 + 4v_{F1}v_{F2}U^2/\pi} \right] \\ (K_{1',2'})^{-2} &= \frac{1}{2v_{F1}v_{F2}} \left[v_{F1}(v_{F1} + V_1/\pi) + v_{F2}(v_{F2} + V_2/\pi) \right. \\ &\quad \left. \mp \sqrt{[v_{F2}(v_{F2} + V_2/\pi) - v_{F1}(v_{F1} + V_1/\pi)]^2 + 4v_{F1}v_{F2}U^2/\pi} \right]. \end{aligned} \quad (\text{A.23})$$

In the $SU(2)$ symmetric case, $v_{F1} = v_{F2}$, $V_1 = V_2 = U/2 = V$, $r = 1$, $\alpha = \pi/4$, Eq. (A.23) reduces to:

$$\begin{aligned} (u_{1',2'})^2 &= [v_F(v_F + V/\pi) \mp v_F V/\pi] \\ (K_{1',2'})^{-2} &= \frac{1}{v_F} [v_F(v_F + V/\pi) \mp v_F V/\pi]. \end{aligned} \quad (\text{A.24})$$

In this case, we may identify θ'_1 with the spin boson θ_σ and θ'_2 with the charge boson, θ_ρ . We see that the Luttinger parameter of the spin boson takes the free fermion value, $K'_1 = K_\sigma = 1$ in the $SU(2)$ symmetric case and the spin velocity is also unaffected by interactions. On the other hand the Luttinger parameter decreases, and the velocity increases for the charge boson.

To understand what may happen when $U > U_c$, note that from Eqs. (A.17), $u'_1/K'_1 < 0$ in this case. The terms in the Hamiltonian involving the θ_j fields may be written in terms of the densities:

$$\rho'_1 \equiv r^{-1} \cos \alpha \rho_1 - r \sin \alpha \rho_2 \quad (\text{A.25})$$

$$\rho'_2 \equiv r^{-1} \sin \alpha \rho_1 + r \cos \alpha \rho_2 \quad (\text{A.26})$$

as

$$H_\theta = \frac{\pi}{2} \sum_j u'_j (K'_j)^{-1} (\rho'_j)^2. \quad (\text{A.27})$$

When $u'_1(K'_1)^{-1} < 0$, it becomes necessary to include terms of higher order in ρ_i in the Hamiltonian for stability. The vanishing of the quadratic term may be associated with a phase transition. A mean field Landau theory analysis suggests, for equivalent channels corresponding to spinful fermions in zero magnetic field, a continuous transition to a ferromagnetic state at $U = U_c$. For inequivalent channels corresponding to spinful fermions in a finite field, Landau theory predicts a first order transition, corresponding to a jump in the magnetization and density, at a value of U less than the value U_c where $u'_1(K'_1)^{-1}$ vanishes.

Appendix B. Renormalization group equations

In this Appendix we derive the cubic term in the RG equations of Eq. (29), setting $\epsilon_i = 0$. Our technique for deriving RG equations is based on the Operator Product Expansion (OPE). While derivation of quadratic terms in β -functions using the OPE is quite standard [28] we require a generalization of this technique involving unusual 3-point OPE's [29]. In addition, anti-commutation relations of Klein factors and the Majorana mode, Eq. (10), play a crucial role. We begin with the boundary interaction, H_b , of Eq. (15) with the bosonic “vertex operators” normalized as in Eq. (16). Perturbation theory in the t_i is ultra-violet divergent so a cut-off is necessary. Following [28] the cut-off is defined by a “hard core repulsion” in perturbation theory. The n^{th} order term in perturbation theory for the partition function has the form:

$$Z_n/Z_0 = \frac{(-1)^n}{n!} \int_{-\beta/2}^{\beta/2} d\tau_1 d\tau_2 \dots d\tau_n \mathcal{T} < H_b(\tau_1) H_b(\tau_2) \dots H_b(\tau_n) >. \quad (\text{B.1})$$

Here we work in imaginary time and \mathcal{T} represents time-ordering while β is the inverse temperature. We will eventually take $\beta \rightarrow \infty$; it just acts as an infrared regulator in the calculation. Below we use the zero temperature Green's functions with that limit in mind. We use the fact that the interaction term in the imaginary time action is simply $S_{\text{int}} = \int d\tau H_b(\tau)$. We may think of $< \dots >$ as representing a Feynman path integral over the bosonic fields. On the other hand, it is more convenient to take the elementary traces over the Majorana mode and Klein factors directly. Ultra-violet divergences occur when two or more of the τ_i approach each other. Our ultra-violet cut-off is to restrict the integration in Eq. (B.1) by requiring $|\tau_i - \tau_j| \geq \tau_0$ for all $i \neq j$. Our basic RG step is to increase the short-time cut-off:

$$\tau_0 \rightarrow \tau_0 + \delta\tau \quad (\text{B.2})$$

corresponding to reducing a cut-off in energy domain. We study how the renormalized parameters t_i change under this increase of τ_0 . This is done using the 3-point OPE of boundary operators:

$$\mathcal{T} [H_b(\tau_1) H_b(\tau_2) H_b(\tau_3)] \rightarrow \sum_{n=1}^{\infty} f_n(\tau_2 - \tau_1, \tau_3 - \tau_1) \mathcal{O}_n(\tau_1). \quad (\text{B.3})$$

Here the limit is taken where τ_1 , τ_2 and τ_3 approach each other. The operators \mathcal{O}_n on the right hand side of Eq. (B.3) are a complete set of boundary operators and the f_n 's are a set of functions, cubic in the t_j 's, which generally become singular when any two τ_i 's become equal. We insert this expansion into the cubic term in Eq. (B.1), obtaining a correction to the effective action. We examine how this correction to the action changes under a small change in τ_0 , extract the term linear in $\delta\tau$ and from this obtain the renormalization of the coupling constants t_i which is cubic in the t_i 's and linear in $\delta\tau$. In doing this, we must be careful to subtract a term which is simply H_b times a perturbation to the free energy of quadratic order in H_b . Thus we may write, in cubic order:

$$\delta S = \frac{1}{3!} \int d\tau_1 d\tau_2 d\tau_3 \sum_{n=1}^{\infty} f_n(\tau_2 - \tau_1, \tau_3 - \tau_1) \mathcal{O}_n(\tau_1)$$

$$- \int d\tau_1 H_b(\tau_1) \frac{1}{2!} \int d\tau_2 d\tau_3 \mathcal{T} < H_b(\tau_2) H_b(\tau_3) > . \quad (\text{B.4})$$

The last term in Eq. (B.4) cancels many of the contributions from the first one.

The OPE in Eq. (B.3) factorizes into contributions from the Majorana modes, Klein factors and bosonic operators. Using the defining anti-commutation relations of Eq. (10), we obtain for the Majorana modes:

$$\mathcal{T} [\gamma(\tau_1) \gamma(\tau_2) \gamma(\tau_3)] = \epsilon(\tau_1, \tau_2, \tau_3) \gamma \quad (\text{B.5})$$

where ϵ is the anti-symmetric step function of 3 arguments:

$$\begin{aligned} \epsilon(\tau_1, \tau_2, \tau_3) &= 1, \quad (\tau_1 > \tau_2 > \tau_3) \\ &= -1 \quad (\tau_2 > \tau_1 > \tau_3) \end{aligned} \quad (\text{B.6})$$

et cetera. Note that the operator γ doesn't actually have any time dependence in perturbation theory since it doesn't appear in the unperturbed Hamiltonian. The time-dependence in Eq. (B.6) arises from the time-ordering due to the anti-commutation relations. Similarly:

$$\mathcal{T} [\Gamma_1(\tau_1) \Gamma_1(\tau_2) \Gamma_1(\tau_3)] = \epsilon(\tau_1, \tau_2, \tau_3) \Gamma_1. \quad (\text{B.7})$$

By contrast:

$$\mathcal{T} [\Gamma_1(\tau_1) \Gamma_1(\tau_2) \Gamma_2(\tau_3)] = \epsilon(\tau_1 - \tau_2) \Gamma_2 \quad (\text{B.8})$$

where $\epsilon(\tau)$ is the standard anti-symmetric step function. Of course, the analogous equations hold with the indices 1 and 2 interchanged. To calculate the 3-point OPE of bosonic operators, we first consider the 4-point function for a boson field $\phi(\tau) \equiv \phi(\tau, x=0)$, with the Hamiltonian

$$H = \frac{u}{2} \int_0^\infty dx \left[K \left(\frac{\partial \phi}{\partial x} \right)^2 + K^{-1} \left(\frac{\partial \theta}{\partial x} \right)^2 \right]. \quad (\text{B.9})$$

Using standard Gaussian path integration techniques and the normalization of Eq. (16), this is:

$$\mathcal{T} < e^{i\sqrt{\pi}\phi(\tau_1)} e^{i\sqrt{\pi}\phi(\tau_2)} e^{-i\sqrt{\pi}\phi(\tau_3)} e^{-i\sqrt{\pi}\phi(\tau_4)} > = \left| \frac{\tau_{12}\tau_{34}}{\tau_{13}\tau_{14}\tau_{23}\tau_{24}} \right|^{\frac{1}{K}} \quad (\text{B.10})$$

where we have defined, for convenience,

$$\tau_{ij} \equiv \tau_i - \tau_j. \quad (\text{B.11})$$

We now consider the limit $\tau_4 \rightarrow \infty$ to extract the 3-point OPE. In this limit, Eq. (B.10) becomes:

$$\begin{aligned} \mathcal{T} < e^{i\sqrt{\pi}\phi(\tau_1)} e^{i\sqrt{\pi}\phi(\tau_2)} e^{-i\sqrt{\pi}\phi(\tau_3)} e^{-i\sqrt{\pi}\phi(\tau_4)} > &\rightarrow \left| \frac{\tau_{12}}{\tau_{13}\tau_{23}} \right|^{\frac{1}{K}} \left| \frac{1}{\tau_4} \right|^{\frac{1}{K}} \\ &= \left| \frac{\tau_{12}}{\tau_{13}\tau_{23}} \right|^{\frac{1}{K}} < e^{i\sqrt{\pi}\phi(\tau_1)} e^{-i\sqrt{\pi}\phi(\tau_3)} > . \end{aligned} \quad (\text{B.12})$$

Thus we deduce the basic OPE:

$$\mathcal{T} \left[e^{i\sqrt{\pi}\phi(\tau_1)} e^{i\sqrt{\pi}\phi(\tau_2)} e^{-i\sqrt{\pi}\phi(\tau_3)} \right] \rightarrow \left| \frac{\tau_{12}}{\tau_{13}\tau_{23}} \right|^{\frac{1}{K}} e^{i\sqrt{\pi}\phi(\tau_1)}. \quad (\text{B.13})$$

This result holds up to higher dimensions operators which are also generated in the effective action, but are not of interest to us. Note that whether the argument of ϕ on the right hand side is chosen to be τ_1 , τ_2 or τ_3 is immaterial, neglecting these higher dimension operators. Eq. (B.13) implies the useful result:

$$\begin{aligned} & \mathcal{T}\{\cos[\sqrt{\pi}\phi(\tau_1)]\cos[\sqrt{\pi}\phi(\tau_2)]\cos[\sqrt{\pi}\phi(\tau_3)]\} \\ & \rightarrow \frac{1}{4}\cos[\sqrt{\pi}\phi(\tau_1)]\left[\left|\frac{\tau_{12}}{\tau_{13}\tau_{23}}\right|^{\frac{1}{K}} + \left|\frac{\tau_{13}}{\tau_{12}\tau_{23}}\right|^{\frac{1}{K}} + \left|\frac{\tau_{23}}{\tau_{12}\tau_{13}}\right|^{\frac{1}{K}}\right]. \end{aligned} \quad (\text{B.14})$$

For two independent bosons, ϕ_1 and ϕ_2 with the bulk Hamiltonian of Eq. (11) we use the trivial result:

$$\mathcal{T}\left\{\cos[\sqrt{\pi}\phi_1(\tau_1)]\cos[\sqrt{\pi}\phi_2(\tau_2)]\cos[\sqrt{\pi}\phi_2(\tau_3)]\right\} \rightarrow \frac{1}{2}\left|\frac{1}{\tau_{23}}\right|^{\frac{1}{K_2}}\cos[\sqrt{\pi}\phi_1(\tau_1)] \quad (\text{B.15})$$

up to higher dimension operators. We can extend these results immediately to the general case discussed in Sec. II with inter-channel coupling. Using the fact that ϕ_ρ and ϕ_σ commute, we simply factorize all exponentials of sums:

$$\exp[i(a\phi_\rho + b\phi_\sigma)] = \exp[ia\phi_\rho]\exp[ib\phi_\sigma] \quad (\text{B.16})$$

and use Eqs. (B.14) and (B.15) with ϕ_1 and ϕ_2 replaced by ϕ_ρ and ϕ_σ and K_1 and K_2 replaced by K_ρ and K_σ . Note that the bosonic OPE's all give positive functions of the τ_i 's whereas the fermionic ones give factors of ± 1 , contributing crucial minus signs.

Let us begin with the T-junction case, of decoupled channels. In this case, since we are taking the limit $\epsilon_i = 0$ for this calculation, we have $1/K_1 = 1/K_2 = 2$. It can be seen that the cubic β -functions contain no terms proportional to t_1^3 or t_2^3 . To obtain this result, first note that Eqs. (B.6) and (B.7) imply the time-independent result:

$$\mathcal{T}[\gamma(\tau_1)\Gamma_1(\tau_1)\gamma(\tau_2)\Gamma_1(\tau_2)\gamma(\tau_3)\Gamma_1(\tau_3)] = -\gamma\Gamma_1. \quad (\text{B.17})$$

Inserting Eq. (B.14) into Eq. (B.4) then gives the term in δS which is cubic in t_1 :

$$\begin{aligned} \delta S^{111} = & -it_1^3 \int d\tau_1 \gamma \Gamma_1 \cos[\sqrt{\pi}\phi_1(\tau_1)] \int d\tau_2 d\tau_3 \left\{ \frac{1}{3!} 2 \left[\left| \frac{\tau_{12}}{\tau_{13}\tau_{23}} \right|^2 \right. \right. \\ & \left. \left. + \left| \frac{\tau_{13}}{\tau_{12}\tau_{23}} \right|^2 + \left| \frac{\tau_{23}}{\tau_{12}\tau_{13}} \right|^2 \right] - 2 \left| \frac{1}{\tau_{23}} \right|^2 \right\} \end{aligned} \quad (\text{B.18})$$

Now we use the remarkable identity

$$\left(\frac{\tau_{12}}{\tau_{13}\tau_{23}}\right)^2 + \left(\frac{\tau_{13}}{\tau_{12}\tau_{23}}\right)^2 + \left(\frac{\tau_{23}}{\tau_{12}\tau_{13}}\right)^2 = 2 \left[\left(\frac{1}{\tau_{12}}\right)^2 + \left(\frac{1}{\tau_{13}}\right)^2 + \left(\frac{1}{\tau_{23}}\right)^2 \right]. \quad (\text{B.19})$$

This can be verified by inspection but can be understood in a deeper way explained in Appendix C. Using Eq. (B.19) we may write:

$$\begin{aligned} \delta S^{111} = & -\frac{2it_1^3}{3} \int d\tau_1 \gamma \Gamma_1 \cos[\sqrt{\pi}\phi_1(\tau_1)] \int d\tau_2 d\tau_3 \left[\left(\frac{1}{\tau_{12}}\right)^2 + \left(\frac{1}{\tau_{13}}\right)^2 \right. \\ & \left. - 2 \left(\frac{1}{\tau_{23}}\right)^2 \right] \theta(|\tau_{12}| - \tau_0) \theta(|\tau_{23}| - \tau_0) \theta(|\tau_{13}| - \tau_0) \end{aligned} \quad (\text{B.20})$$

where in the last line we have inserted explicitly the ultra-violet cut-off which was previously not explicitly written. [$\theta(\tau)$ is the Heaviside step function.] The change in t_1 under a small change in the cut-off, τ_0 is proportional to:

$$\frac{d}{d\tau_0} \int d\tau_2 d\tau_3 \left[\left(\frac{1}{\tau_{12}} \right)^2 + \left(\frac{1}{\tau_{13}} \right)^2 - 2 \left(\frac{1}{\tau_{23}} \right)^2 \right] \theta(|\tau_{12}| - \tau_0) \theta(|\tau_{23}| - \tau_0) \theta(|\tau_{13}| - \tau_0). \quad (\text{B.21})$$

Using:

$$\frac{d}{d\tau_0} \theta(|\tau| - \tau_0) = - \sum_{\pm} \delta(\tau_0 \pm \tau) \quad (\text{B.22})$$

this derivative is a sum of 3 terms, from differentiating each of the step functions. For example, the contribution from differentiating $\theta(|\tau_{12}| - \tau_0)$ is:

$$\begin{aligned} & - \sum_{\pm} \int d\tau_3 \left[\left(\frac{1}{\tau_0} \right)^2 + \left(\frac{1}{\tau_{13}} \right)^2 - 2 \left(\frac{1}{\tau_{13} \pm \tau_0} \right)^2 \right] \theta(|\tau_{13} \pm \tau_0| - \tau_0) \theta(|\tau_{13}| - \tau_0) \\ & \approx - \frac{2\beta}{\tau_0^2} + \frac{3}{\tau_0} \end{aligned} \quad (\text{B.23})$$

up to negligible terms of $O(\tau_0/\beta)$. Adding together the contributions from differentiating the 3 step functions, we obtain zero (up to negligible terms).

Now let us consider the term in δS proportional to $t_1 t_2^2$. The bosonic part of the calculation is much simpler, using Eq. (B.15). There is an essential complication in the fermion part however:

$$\begin{aligned} \mathcal{T} [\gamma(\tau_1) \Gamma_1(\tau_1) \gamma(\tau_2) \Gamma_2(\tau_2) \gamma(\tau_3) \Gamma_2(\tau_3)] &= - \epsilon(\tau_1, \tau_2, \tau_3) \epsilon(\tau_2 - \tau_3) \gamma \Gamma_1 \\ &= - \epsilon(\tau_1 - \tau_2) \epsilon(\tau_1 - \tau_3) \gamma \Gamma_1. \end{aligned} \quad (\text{B.24})$$

Thus we obtain

$$\delta S^{122} = -i \frac{4t_1 t_2^2}{2!} \int d\tau_1 \gamma \Gamma_1 \cos[\sqrt{\pi} \phi_1(\tau_1)] \int d\tau_2 d\tau_3 \left(\frac{1}{\tau_{23}} \right)^2 [\epsilon(\tau_1 - \tau_2) \epsilon(\tau_1 - \tau_3) - 1]. \quad (\text{B.25})$$

Note this is non-zero only due to the sign functions coming from the Majorana mode and Klein factors. We may rewrite this as:

$$\delta S^{122} = i 8 t_1 t_2^2 \int d\tau_1 \gamma \Gamma_1 \cos[\sqrt{\pi} \phi_1(\tau_1)] \int_{-\beta/2}^{\tau_1 - \tau_0} d\tau_2 \int_{\tau_1 + \tau_0}^{\beta/2} d\tau_3 \left(\frac{1}{\tau_{23}} \right)^2. \quad (\text{B.26})$$

Up to terms which are negligible at $\beta \rightarrow \infty$, $\tau_0 \rightarrow 0$, this becomes:

$$\delta S^{122} = i 8 t_1 t_2^2 \ln(\beta/\tau_0) \int d\tau_1 \gamma \Gamma_1 \cos[\sqrt{\pi} \phi_1(\tau_1)]. \quad (\text{B.27})$$

Thus:

$$\frac{d}{d\tau_0} \delta S^{122} = -i \frac{8 t_1 t_2^2}{\tau_0} \int d\tau_1 \gamma \Gamma_1 \cos[\sqrt{\pi} \phi_1(\tau_1)]. \quad (\text{B.28})$$

This determines the cubic term in the β -function:

$$\frac{dt_1}{d \ln \tau_0} = -4 t_1 t_2^2. \quad (\text{B.29})$$

Referring to Eqs. (28,29), we see that we have proven $\mathcal{F}(0) = 4$.

We now consider the general case, discussed in Sec. II. Using Eq. (12), we have:

$$\begin{aligned} & \mathcal{T} \left[8 \cos[\sqrt{\pi}\phi_1(\tau_1)] \cos[\sqrt{\pi}\phi_2(\tau_2)] \cos[\sqrt{\pi}\phi_2(\tau_3)] \right] \\ &= \sum_{s_i=\pm 1} \mathcal{T} \exp \left\{ i\sqrt{\pi} \left[s_1 r^{-1} \cos \alpha \phi_\sigma(\tau_1) - i r \sin \alpha [s_2 \phi_\sigma(\tau_2) + s_3 \phi_\sigma(\tau_3)] \right] \right\} \\ & \times \mathcal{T} \exp \left\{ i\sqrt{\pi} \left[s_1 r^{-1} \sin \alpha \phi_\rho(\tau_1) + i r \cos \alpha [s_2 \phi_\rho(\tau_2) + s_3 \phi_\rho(\tau_3)] \right] \right\}. \end{aligned} \quad (\text{B.30})$$

Only the terms with $s_3 = -s_2$ will renormalize the original couplings. Then we use the OPE's, derived as above:

$$\begin{aligned} & \mathcal{T} \exp \left\{ i\sqrt{\pi} \left[s_1 r^{-1} \cos \alpha \phi_\sigma(\tau_1) - i r \sin \alpha [s_2 \phi_\sigma(\tau_2) + s_3 \phi_\sigma(\tau_3)] \right] \right\} \\ & \rightarrow \exp[i s_1 r^{-1} \cos \alpha \sqrt{\pi} \phi_\sigma(\tau_1)] \left| \frac{\tau_{13}}{\tau_{12}} \right|^{s_1 s_2 \cos \alpha \sin \alpha / K_\sigma} \left| \frac{1}{\tau_{23}} \right|^{r^2 \sin^2 \alpha / K_\sigma} \end{aligned} \quad (\text{B.31})$$

and

$$\begin{aligned} & \mathcal{T} \exp \left\{ i\sqrt{\pi} \left[s_1 r^{-1} \sin \alpha \phi_\rho(\tau_1) + i r \cos \alpha [s_2 \phi_\rho(\tau_2) + s_3 \phi_\rho(\tau_3)] \right] \right\} \\ & \rightarrow \exp[i s_1 r^{-1} \sin \alpha \sqrt{\pi} \phi_\rho(\tau_1)] \left| \frac{\tau_{12}}{\tau_{13}} \right|^{s_1 s_2 \cos \alpha \sin \alpha / K_\rho} \left| \frac{1}{\tau_{23}} \right|^{r^2 \cos^2 \alpha / K_\rho}. \end{aligned} \quad (\text{B.32})$$

Using Eqs. (27), we obtain:

$$\begin{aligned} & \mathcal{T} \left[8 \cos[\sqrt{\pi}\phi_1(\tau_1)] \cos[\sqrt{\pi}\phi_2(\tau_2)] \cos[\sqrt{\pi}\phi_2(\tau_3)] \right] \\ & \rightarrow 2 \cos[\sqrt{\pi}\phi_1(\tau_1)] \left(\frac{1}{\tau_{23}} \right)^2 \left[\left| \frac{\tau_{12}}{\tau_{13}} \right|^\nu + \left| \frac{\tau_{13}}{\tau_{12}} \right|^\nu \right] \end{aligned} \quad (\text{B.33})$$

where ν is defined in Eq. (28). Therefore Eq. (B.25) is modified to:

$$\begin{aligned} \delta S^{122} &= -i \frac{2t_1 t_2^2}{2!} \int d\tau_1 \gamma \Gamma_1 \cos[\sqrt{\pi}\phi_1(\tau_1)] \int d\tau_2 d\tau_3 \left(\frac{1}{\tau_{23}} \right)^2 \\ & \times \left[\left(\left| \frac{\tau_{12}}{\tau_{13}} \right|^\nu + \left| \frac{\tau_{13}}{\tau_{12}} \right|^\nu \right) \epsilon(\tau_1 - \tau_2) \epsilon(\tau_1 - \tau_3) - 2 \right]. \end{aligned} \quad (\text{B.34})$$

This gives the β -functions of Eq. (29) with

$$\begin{aligned} \mathcal{F}(\nu) &= \frac{\tau_0}{2} \frac{d}{d\tau_0} \int d\tau_2 d\tau_3 \left(\frac{1}{\tau_{23}} \right)^2 \left[\left(\left| \frac{\tau_{12}}{\tau_{13}} \right|^\nu + \left| \frac{\tau_{13}}{\tau_{12}} \right|^\nu \right) \epsilon(\tau_1 - \tau_2) \epsilon(\tau_1 - \tau_3) - 2 \right] \\ & \times \prod_{i < j} \theta(|\tau_{ij}| - \tau_0). \end{aligned} \quad (\text{B.35})$$

(Note that, by time-translation invariance, this double integral is independent of τ_1 . We will show that this object becomes independent of τ_0 and β in the limit $\tau_0/\beta \rightarrow 0$, that we are considering.) Before evaluating $\mathcal{F}(\nu)$ in general, it is interesting to consider the SU(2) invariant case, $\nu = 1$. Then we can use:

$$\left(\left| \frac{\tau_{12}}{\tau_{13}} \right| + \left| \frac{\tau_{13}}{\tau_{12}} \right| \right) \epsilon(\tau_1 - \tau_2) \epsilon(\tau_1 - \tau_3) - 2 = \frac{\tau_{12}}{\tau_{13}} + \frac{\tau_{13}}{\tau_{12}} - 2 = \frac{\tau_{23}^2}{\tau_{12} \tau_{13}} \quad (\text{B.36})$$

to reduce Eq. (B.35) to:

$$\mathcal{F}(1) = \frac{\tau_0}{2} \frac{d}{d\tau_0} \int d\tau_2 d\tau_3 \frac{1}{\tau_{12} \tau_{13}}. \quad (\text{B.37})$$

This is a product of 2 ultraviolet finite principal value integrals and is consequently independent of the cut-off up to corrections that vanish when $\tau_0 \ll \beta$. Therefore,

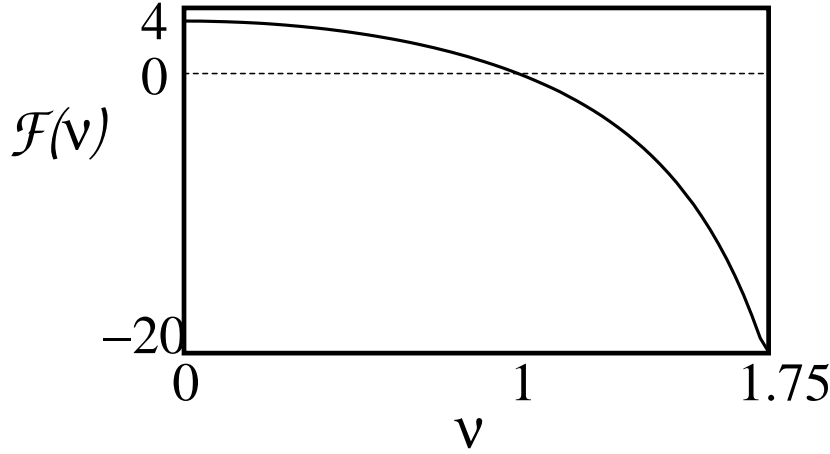


Figure B1. Plot of the function $F(\nu)$ appearing in the β function of Eq. (29).

$\mathcal{F}(1) = 0$, a result that must hold due to SU(2) symmetry as discussed in Sec. II. To simplify Eq. (B.35) in general, we first rewrite it as:

$$\begin{aligned} \mathcal{F}(\nu) = \tau_0 \frac{d}{d\tau_0} \left\{ \int_{\tau_0}^{\beta/2} \frac{d\tau_2 d\tau_3}{\tau_{23}^2} \left[\left(\frac{\tau_2}{\tau_3} \right)^\nu + \left(\frac{\tau_3}{\tau_2} \right)^\nu - 2 \right] \theta(|\tau_{23}| - \tau_0) \right. \\ \left. - \int_{\tau_0}^{\beta/2} \frac{d\tau_2 d\tau_3}{(\tau_2 + \tau_3)^2} \left[\left(\frac{\tau_2}{\tau_3} \right)^\nu + \left(\frac{\tau_3}{\tau_2} \right)^\nu + 2 \right] \right\}. \end{aligned} \quad (\text{B.38})$$

Differentiating the explicit step function in Eq. (B.38) gives:

$$\begin{aligned} - \frac{2}{\tau_0} \int_{\tau_0}^{\beta/2} d\tau_2 \left[\left(\frac{\tau_2 + \tau_0}{\tau_2} \right)^\nu + \left(\frac{\tau_2}{\tau_2 + \tau_0} \right)^\nu - 2 \right] \\ \rightarrow -2 \int_1^\infty dx \left[\left(\frac{x+1}{x} \right)^\nu + \left(\frac{x}{x+1} \right)^\nu - 2 \right] \end{aligned} \quad (\text{B.39})$$

where we have rescaled the integration variable $\tau = \tau_0 x$ and taken $\beta \rightarrow \infty$ in the last expression. Differentiating the lower limits of integration in Eq. (B.38) gives:

$$\begin{aligned} -2\tau_0 \int_{2\tau_0}^{\beta/2} \frac{d\tau_2}{(\tau_2 - \tau_0)^2} \left[\left(\frac{\tau_2}{\tau_0} \right)^\nu + \left(\frac{\tau_0}{\tau_2} \right)^\nu - 2 \right] \\ + 2\tau_0 \int_{\tau_0}^{\beta/2} \frac{d\tau_2}{(\tau_2 + \tau_0)^2} \left[\left(\frac{\tau_2}{\tau_0} \right)^\nu + \left(\frac{\tau_0}{\tau_2} \right)^\nu + 2 \right] \end{aligned} \quad (\text{B.40})$$

Doing the simple integrals exactly, again rescaling the integration variable, taking $\beta \rightarrow \infty$, and collecting terms gives an expression for the needed function $F(\nu)$ in terms of a convergent dimensionless integral:

$$\begin{aligned} \mathcal{F}(\nu) = 6 - 2 \int_1^\infty dx \left[\frac{(x+1)^\nu + (x+1)^{-\nu}}{x^2} - \frac{x^\nu + x^{-\nu}}{(x+1)^2} \right. \\ \left. + \left(\frac{x+1}{x} \right)^\nu + \left(\frac{x+1}{x} \right)^{-\nu} - 2 \right]. \end{aligned} \quad (\text{B.41})$$

We did the integral numerically and $\mathcal{F}(\nu)$ is plotted in Fig. (B1). Note that it is monotone decreasing, with $\mathcal{F}(0) = 4$ and $\mathcal{F}(1) = 0$ as calculated analytically above.

Appendix C. Spin chain representation

A mapping of a tight binding version of our model onto a spin chain Hamiltonian provides intuition about the phase diagram as well as a useful representation for possible future numerical work. This mapping generalizes an approach introduced in [13] for the single channel case. We first represent each channel by a semi-infinite spinless fermion tight-binding chain and represent the two Majorana modes of the superconductor, ψ_S of Eq. (23), by the electron operator at the origin, c_0 . For the T-junction (no inter-channel interactions) the various terms in the Hamiltonian of Eq. (2) become:

$$\begin{aligned} H_0 &= -(J_1/2) \sum_{j=-\infty}^{-2} c_j^\dagger c_{j+1} - (J_2/2) \sum_{j=1}^{\infty} c_j^\dagger c_{j+1} + \text{h.c.} \\ H_{\text{int}} &= V_1 \sum_{j=-\infty}^{-1} (n_j - 1/2)(n_{j-1} - 1/2) + V_2 \sum_{j=1}^{\infty} (n_j - 1/2)(n_{j+1} - 1/2) \\ H_b &= -t_1(c_0^\dagger + c_0)(c_{-1}^\dagger - c_{-1})/2 - t_2(c_0^\dagger + c_0)(c_1^\dagger - c_1)/2. \end{aligned} \quad (\text{C.1})$$

We now make an “inverse Jordan-Wigner transformation” to a set of $S=1/2$ variables on each lattice site:

$$c_j^\dagger c_j = S_j^z + 1/2, \quad c_j = \left[\prod_{l < j} (-2S_l^z) \right] S_j^- . \quad (\text{C.2})$$

The resulting Hamiltonian in terms of spin-1/2 variables, after the transformation $S_j^\pm \rightarrow (-1)^j S_j^\pm$ is:

$$\begin{aligned} H_0 + H_{\text{int}} &= \sum_{j=-\infty}^{-2} [J_1(S_j^x S_{j+1}^x + S_j^y S_{j+1}^y) + V_1 S_j^z S_{j+1}^z] \\ &\quad + \sum_{j=1}^{\infty} [J_2(S_j^x S_{j+1}^x + S_j^y S_{j+1}^y) + V_2 S_j^z S_{j+1}^z] \\ H_b &= -2t_1 S_0^x S_{-1}^x - 2t_2 S_0^y S_1^y. \end{aligned} \quad (\text{C.3})$$

We see that, when $t_1 = t_2 = 0$, we have 2 independent xxz model defined on semi-infinite lines, $j > 0$ and $j < 0$ with the impurity spin at the origin decoupled. Each spin chain obeys “open boundary conditions” at the origin. Turning on t_1 , the chain at $j > 0$ remains decoupled and $[S_0^x, H] = 0$. As discussed in [13], there are 2 equivalent ground states in which $S_0^x = \pm 1/2$. The spin chain defined at $j < 0$ then experiences a boundary magnetic field pointing in the $\pm x$ direction:

$$B_x = \pm t_1. \quad (\text{C.4})$$

This transverse boundary field model was analyzed in [30]. Along the xxz critical line, $0 < V_1/J_1 < 1$, this is a relevant boundary interaction. To see this we may bosonize the two spin chains, introducing bosons (ϕ_j, θ_j) with the bulk Hamiltonian of Eq. (11) and boundary terms:

$$\begin{aligned} H_b &= 2t_1 \tau_0^{-1+d_1} S_0^x \left\{ \exp[i\sqrt{\pi}\phi_1(0)] + \exp[-i\sqrt{\pi}\phi_1(0)] \right\} \\ &\quad + 2t_2 \tau_0^{-1+d_2} S_0^y \left\{ \exp[i\sqrt{\pi}\phi_2(0)] + \exp[-i\sqrt{\pi}\phi_2(0)] \right\}. \end{aligned} \quad (\text{C.5})$$

This Hamiltonian could have been obtained directly from Eq. (15) by the substitution:

$$\begin{aligned} i\gamma\Gamma_1 &\rightarrow 2S_0^x \\ i\gamma\Gamma_2 &\rightarrow 2S_0^y. \end{aligned} \quad (\text{C.6})$$

The conclusion of [30] was that, for $t_2 = 0$, the relevant interaction t_1 renormalizes to large values, pinning $\phi_1(0)$. $\langle S_j^x \rangle$ then becomes non-zero, with power-law decay away from the boundary. This boundary field fixed point of the spin chain corresponds to perfect Andreev reflection in the fermion system an analogy that was discussed in [14]. When t_1 and t_2 are both non-zero, there is a competition between S_0^x and S_0^y being pinned. This frustration leads to the non-trivial critical point discussed in Sec. II.

The case of marginal boundary Hamiltonian, $d_i = 1$, $K_j = 1/2$, corresponds to Heisenberg antiferromagnetic chains, $V_i = J_i$. This leads to new insights into the cubic terms in the β -functions for decoupled chains, $\nu = 0$. In this case the SU(2) symmetry of each spin chain [not to be confused with the SU(2) symmetry discussed earlier in the fermion basis], may be used to rewrite the boundary Hamiltonian as:

$$H_b = 2t_1 S_0^x S_{-1}^z + 2t_2 S_0^y S_1^z. \quad (\text{C.7})$$

Upon bosonizing we obtain:

$$H_b = t'_1 S_0^x \partial_x \phi_1(0) + t'_2 S_0^y \partial_x \phi_2(0) \quad (\text{C.8})$$

for some rescaled boundary couplings t'_i . The equivalence of the operators $\partial_x \phi$ and $\cos \sqrt{\pi} \phi$ in the case $K = 1/2$ follows from the hidden SU(2) symmetry of the bosonized Heisenberg model. It is this hidden symmetry which explains the remarkable identity in Eq. (B.19). Eq. (C.8) was precisely the interaction studied in [19],[20] as a model of a 2 level system with non-commuting interactions with 2 independent heat baths. The cubic RG equations derived in Appendix B of this paper are identical, for $\nu = 0$, to the ones derived by a different method in [19],[20]. Precisely the Hamiltonian of Eq. (C.3), for the case $J_1 = J_2$, $V_1 = V_2$ arbitrary, was studied in [21] as a version of the dissipative Hofstadter model, and the RG equations were analyzed there, following [22] and [23].

The model of Eq. (C.3) also has an interesting connection with the 2-channel Kondo model in the marginal case of Heisenberg chains, $V_1 = J_1 = V_2 = J_2$. The 2-channel Kondo model involves 2 channels of conduction electrons interacting with an impurity spin. Upon bosonizing the low energy effective Hamiltonian, only the spin degrees of freedom of each fermion channel participates in the Kondo interaction. The model then becomes equivalent to two semi-infinite Heisenberg chains with a weak coupling to a central spin. This is again the Hamiltonian of Eq. (C.3) but with H_b replaced by an isotropic version:

$$H_b = 2\vec{S}_0 \cdot [t_1 \vec{S}_1 + t_2 \vec{S}_{-1}]. \quad (\text{C.9})$$

After an appropriate rescaling of the t_i 's this model has a quadratic plus cubic β -function:

$$\frac{dt_j}{dl} = 2t_j^2 - 8t_j \sum_{k=1}^2 t_k^2. \quad (\text{C.10})$$

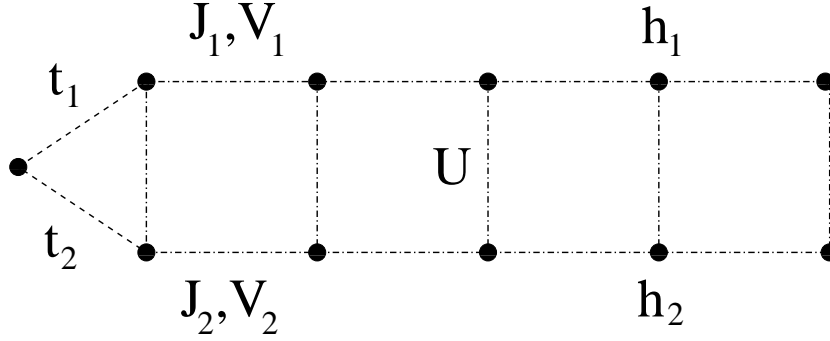


Figure C1. The 2 leg spin ladder coupled to an impurity corresponding to the coupled 2 channel fermion model.

(See [29] for a derivation of this β -function using OPE methods.) Now consider an anisotropic 2-channel Kondo model with:

$$H_b = 2 \sum_{a=x,y,z} S_0^a \cdot [t_1^a S_1^a + t_2^a S_{-1}^a]. \quad (\text{C.11})$$

By a simple extension of the methods in [29] it can be seen that the β -function becomes:

$$\frac{dt_j^a}{dl} = \sum_{b,c} |\epsilon^{abc}| t_j^b t_j^c - 4t_j^a \sum_{b \neq a} \sum_{k=1}^2 t_k^b t_k^b. \quad (\text{C.12})$$

We see that the Majorana interaction of Eq. (C.3) corresponds to $t_1^x = -t_1$, $t_2^y = -t_2$ all other t_i^a 's zero. Then we see that the quadratic terms in the Kondo β -function vanish and the cubic term reduces to the one in our Majorana model.

So far, we have discussed the T-junction case of decoupled channels coupled to a Majorana mode, showing that it maps onto 2 semi-infinite spin chains coupled to an impurity spin. We may extend this mapping to the case of coupled channels. In this case we get an impurity spin end-coupled to a 2-leg spin ladder as sketched in Fig. (C1). Labelling the spins $\vec{S}_{i,j}$ where $i = 1, 2, 3, \dots \infty$ measures distance along the chain and $j = 1, 2$ indexes the 2 legs, the Hamiltonian, after the inverse Jordan-Wigner transformation, becomes:

$$\begin{aligned} H_0 &= \sum_{i=1}^{\infty} \sum_{j=1}^2 [J_j (S_{i,j}^x S_{i+1,j}^x + S_{i,j}^y S_{i+1,j}^y) - h_j S_{i,j}^z] \\ H_{\text{intra}} &= \sum_{i=1}^{\infty} \sum_{j=1}^2 V_j S_{i,j}^z S_{i+1,j}^z \\ H_{\text{inter}} &= U \sum_{i=1}^{\infty} S_{i,1}^z S_{i,2}^z \\ H_b &= -2t_1 S_0^x S_{1,1}^x - 2t_2 S_0^y S_{1,2}^y. \end{aligned} \quad (\text{C.13})$$

We have added unequal magnetic fields, $h_1 \neq h_2$, acting on the 2 legs, in order to avoid developing a gap, as discussed in Sec. II.

These one dimensional spin chain models could be readily studied using either Density Matrix Renormalization Group or Quantum Monte Carlo. (The spin chain

version developed in this Appendix makes it clear there is no fermion sign problem.) This would be very useful for checking our conjectured phase diagram and, in particular, the existence and properties of the non-trivial critical point.

Appendix D. $A \otimes N$ fixed point

As discussed in Sec. II, our RG equations, for $0 < \epsilon_i \ll 1$, indicate that the only stable fixed points are $A \otimes N$ (and $N \otimes A$). In this Appendix we investigate the stability and other properties of this fixed point in more detail. These are characterized by the conformally invariant boundary conditions:

$$\begin{aligned}\phi_1(0) &= 0 \text{ or } \sqrt{\pi} \\ \theta_2(0) &= 0 \text{ or } \sqrt{\pi}.\end{aligned}\tag{D.1}$$

In the T-junction case, where channels 1 and 2 are decoupled, the properties of these fixed points are well-known. As for the normal reflection boundary condition, the starting point of our analysis in Sec. II, the channel-two fermion fields at the junction are bosonized as:

$$\psi_2(0) \propto \exp[i\sqrt{\pi}\phi_2(0)], \quad \psi_2^\dagger(0) \propto \exp[-i\sqrt{\pi}\phi_2(0)],\tag{D.2}$$

giving operators of dimension $d_2 = 1/(2K_2)$. On the other hand, we see from Eq. (9) and (D.1) that the channel-one fermion fields at the junction are bosonized as:

$$\psi_1(0) = \psi_1^\dagger(0) \propto \cos[\sqrt{\pi}\theta_1(0)]\tag{D.3}$$

of dimension $d_{A1} = K_1/2$. From these results we can work out the dimensions of the various boundary operators at this fixed point. Normal reflection in channel 1 corresponds to

$$\psi_1^\dagger(0)\psi_1(0) \propto \cos[2\sqrt{\pi}\theta_1(0)]\tag{D.4}$$

of dimension $2K_1$. This is $1/d_1$ where d_1 is the dimension of the coupling to the Majorana mode analyzed in Sec. II. Thus, whenever that Majorana coupling is relevant, and the system flows to the $A \otimes N$ fixed point, this normal scattering is irrelevant.

We now consider Andreev scattering in channel 2 at the $A \otimes N$ fixed point, corresponding to the perturbation analysed in Sec. II

$$H_{b2} \equiv 2it_2\tau_0^{-1+d_2}\gamma\Gamma_2 \cos[\sqrt{\pi}\phi_2(0)].\tag{D.5}$$

In analyzing the effect of this operator it is important to take into account the ‘‘Schrodinger cat’’ nature of the $A \otimes N$ ground states, as discussed in Sec. II. Ignoring channel 2, there are 2 ground states in which $i\gamma\Gamma_1 = \pm 1$ and correspondingly $\langle \cos \sqrt{\pi}\phi_1(0) \rangle$ is negative or positive. The localized Dirac state constructed from γ and Γ_1 is occupied or empty in these 2 states respectively. The operator $\gamma\Gamma_2$ acts off-diagonally in the local mode space since

$$\gamma = \psi_0 + \psi_0^\dagger\tag{D.6}$$

where ψ_0 , defined in Eq. (22), annihilates the local mode state. Therefore acting with H_{b2} on one of these states produces a high energy state where the local mode occupancy is switched without changing the sign of $\langle \cos \sqrt{\pi} \phi_1(0) \rangle$ (i.e. without changing the electron number parity in channel 1). We thus should treat H_{b2} using a ‘‘Schrieffer-Wolff’’ type procedure [31], familiar from the mapping of the Anderson impurity model into the Kondo model. The perturbation then corresponds to

$$\delta H \propto \frac{t_2^2}{t_1} [\psi_2^\dagger \partial_x \psi_2^\dagger + h.c.] \propto \frac{t_2^2}{t_1} \cos[2\sqrt{\pi} \phi_2(0)]. \quad (\text{D.7})$$

Low energy processes can only transfer pairs of electrons between channel 2 and the superconductor, to avoid changing the occupancy of the local mode. This simply corresponds to regular Andreev scattering processes that could take place without the presence of the Majorana mode. Once the Majorana mode is strongly entangled with channel 1, it cannot enable Andreev scattering in channel 2. The perturbation in Eq. (D.7) has dimension $2/K_2 = 4d_2$ and is thus strongly irrelevant.

Finally, we must consider processes that change the number of electrons in each channel by ± 1 . These can either correspond to Andreev tunnelling of a pair of electrons, one drawn from each channel, into (or out of) the superconductor or to transfer of a single electron between the 2 channels. In this case, the Schrieffer-Wolff transformation is not necessary and a representative operator is:

$$H_{12} \propto \psi_1(0) \psi_2(0) \propto \cos[\sqrt{\pi} \theta_1(0)] \exp[i\sqrt{\pi} \phi_2(0)] \quad (\text{D.8})$$

of dimension:

$$d = d_{A1} + d_2 = \frac{1}{2} \left(K_1 + \frac{1}{K_2} \right). \quad (\text{D.9})$$

This is irrelevant, $d > 1$, when $K_1 = K_2 < 1$ corresponding to equal repulsive interactions in both channels. However, it can be relevant when $K_1 < K_2 < 1$, to the left of the line $K_1 = 2 - 1/K_2$. This is physically reasonable. If channel 1 has stronger repulsive interactions than channel 2 then the fixed point with perfect Andreev scattering in channel 1 and perfect normal scattering in channel 2 can become unstable. Taking into account the stability conditions at $A \otimes N$, $N \otimes A$ and $N \otimes N$ fixed points, we can identify 6 different regions in the K_1 - K_2 plane, with $K_i < 1$, which have different phase diagrams and RG flows in the t_1 - t_2 plane. These regions are numbered in Fig. (D1a). In Table (D1) the fixed points are indicated which are either stable or semi-stable (meaning stable under moving in precisely one direction in the t_1 - t_2 plane) in each of these 6 regions. In Fig. (D1b), a qualitative sketch of the RG flow diagram is given for a point in region 2.

We now consider the case with inter-channel interactions, which is a rather novel fixed point. It’s properties were discussed in [13] using the technique of integrating out the boson fields everywhere except at the origin. Here we wish to discuss this fixed point using boundary conformal field theory (BCFT) techniques where a conformally invariant boundary condition is applied to the bulk conformal field theory of 2 free bosons. We will corroborate some of the conclusions of [13] as well as gaining new insight. The

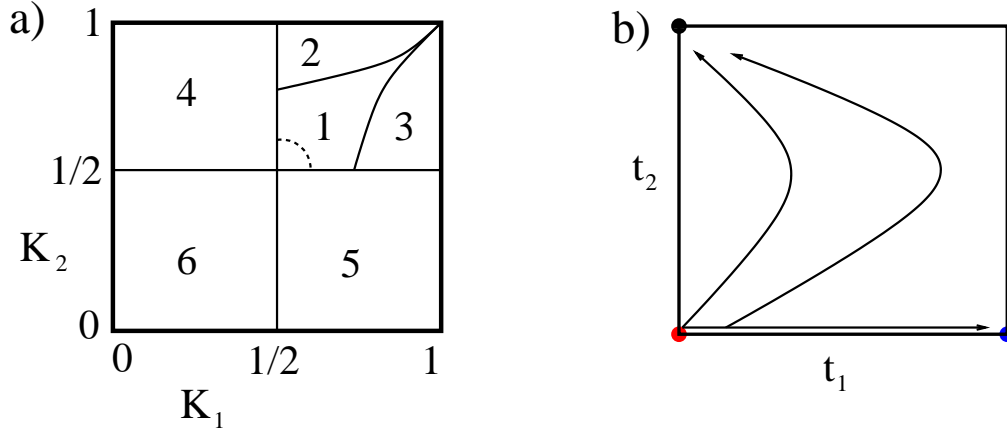


Figure D1. a): Sketch of various regions in the K_1 - K_2 plane which have different phase diagrams and RG flows in the t_1 - t_2 plane, for the T -junction (decoupled channels). The dashed quarter-circle indicates qualitatively the parameter region where the ϵ -expansion is valid and predicts a NTCP. b): Qualitative sketch of the RG flow in region 2.

Region	Stable	Semi-stable
1	$A \otimes N, N \otimes A$	NTCP
2	$N \otimes A$	$A \otimes N$
3	$A \otimes N$	$N \otimes A$
4	$N \otimes A$	$N \otimes N$
5	$A \otimes N$	$N \otimes N$
6	$N \otimes N$	—

Table D1. Stable and semi-stable fixed points in different regions of K_1 - K_2 plane for the T -junction (decoupled channels). The six regions are labelled as in Fig. (D1).

BCFT approach is generally more powerful since it lends itself to calculating Green's functions at arbitrary spatial locations as well as the impurity entropy, which we discuss in Appendix G.

When both couplings to the Majorana mode are turned off, $t_1 = t_2 = 0$, the boson fields obey the boundary conditions $\theta_1(0) = \theta_2(0) = 0$. However, when t_1 renormalizes to large values and t_2 renormalizes to zero, we expect a new boundary condition, from Eq. (12):

$$\cos \alpha \phi_\sigma(0) + \sin \alpha \phi_\rho(0) = 0 \text{ or } r\sqrt{\pi} \quad (\text{D.10})$$

which couples the independent boson fields ϕ_ρ and ϕ_σ with different Luttinger

parameters. This is only a partial specification of a conformally invariant boundary condition; we wish to deduce the complementary condition. To do this, it is convenient to first rewrite the Hamiltonian in terms of rescaled fields:

$$\bar{\phi}_\lambda \equiv \sqrt{K_\lambda} \phi_\lambda, \quad \bar{\theta}_\lambda \equiv \theta_\lambda / \sqrt{K_\lambda}. \quad (\text{D.11})$$

Note that these obey canonical commutation relations:

$$[\bar{\phi}_\lambda(x), \bar{\theta}_{\lambda'}(y)] = -\frac{i}{2} \delta_{\lambda, \lambda'} \epsilon(x - y). \quad (\text{D.12})$$

The Hamiltonian of Eq. (13) now takes the simple form:

$$H = \frac{1}{2} \sum_\lambda u_\lambda \int dx [(\partial_x \bar{\phi}_\lambda)^2 + (\partial_x \bar{\theta}_\lambda)^2]. \quad (\text{D.13})$$

It is now convenient to rescale distance, x , differently for the ρ and σ fields:

$$\tilde{\phi}_\lambda(x/u_\lambda) \equiv \bar{\phi}_\lambda(x), \quad \tilde{\theta}_\lambda(x/u_\lambda) \equiv \bar{\theta}_\lambda(x). \quad (\text{D.14})$$

The Hamiltonian can then be written:

$$H = \frac{1}{2} \sum_\lambda \int dx [(\partial_x \tilde{\phi}_\lambda)^2 + (\partial_x \tilde{\theta}_\lambda)^2] \quad (\text{D.15})$$

where the x integration variable now has dimensions of time. Next, we make a canonical transformation, motivated by pinning of $\frac{\cos \alpha}{\sqrt{K_\sigma}} \tilde{\phi}_\sigma(0) + \frac{\sin \alpha}{\sqrt{K_\rho}} \tilde{\phi}_\rho(0)$:

$$\begin{pmatrix} \phi'_1 \\ \phi'_2 \end{pmatrix} = \mathcal{O} \begin{pmatrix} \tilde{\phi}_\sigma \\ \tilde{\phi}_\rho \end{pmatrix}, \quad \begin{pmatrix} \theta'_1 \\ \theta'_2 \end{pmatrix} = \mathcal{O} \begin{pmatrix} \tilde{\theta}_\sigma \\ \tilde{\theta}_\rho \end{pmatrix} \quad (\text{D.16})$$

where \mathcal{O} is the orthogonal matrix:

$$\mathcal{O} = \frac{1}{\sqrt{\cos^2 \alpha K_\rho + \sin^2 \alpha K_\sigma}} \begin{pmatrix} \cos \alpha \sqrt{K_\rho} & \sin \alpha \sqrt{K_\sigma} \\ -\sin \alpha \sqrt{K_\sigma} & \cos \alpha \sqrt{K_\rho} \end{pmatrix}. \quad (\text{D.17})$$

The Hamiltonian still takes the canonical form of Eq. (D.15) in this basis and our conformally invariant boundary conditions simply correspond to pinning $\phi'_1(0)$ and $\theta'_2(0)$. To work out the scaling dimensions of the various boundary operators at the $A \otimes N$ fixed point, we express the original fields ϕ_i and θ_i at the origin in terms of the transformed fields:

$$\begin{aligned} \phi_1(0) &= r^{-1} \sqrt{\frac{\cos^2 \alpha K_\rho + \sin^2 \alpha K_\sigma}{K_\rho K_\sigma}} \phi'_1(0) \\ \phi_2(0) &= r \left[\frac{(K_\sigma - K_\rho) \sin 2\alpha}{\sqrt{4K_\rho K_\sigma (\cos^2 \alpha K_\rho + \sin^2 \alpha K_\sigma)}} \phi'_1(0) + \frac{1}{\sqrt{\cos^2 \alpha K_\rho + \sin^2 \alpha K_\sigma}} \phi'_2(0) \right] \\ \theta_1(0) &= r \left[\sqrt{\frac{K_\rho K_\sigma}{\cos^2 \alpha K_\rho + \sin^2 \alpha K_\sigma}} \theta'_1(0) + \frac{\sin 2\alpha (K_\rho - K_\sigma)}{\sqrt{4(\cos^2 \alpha K_\rho + \sin^2 \alpha K_\sigma)}} \theta'_2(0) \right] \\ \theta_2(0) &= r^{-1} \sqrt{\cos^2 \alpha K_\rho + \sin^2 \alpha K_\sigma} \theta'_2(0). \end{aligned} \quad (\text{D.18})$$

Using the conditions that $\phi'_1(0)$ and $\theta'_2(0)$ are pinned, together with Eq. (D.18), may now read off the dimensions of the various boundary operators. Normal back-scattering in channel 1 gives

$$\psi_{1L}^\dagger(0)\psi_{1R}(0) \propto e^{2i\sqrt{\pi}\theta_1} \propto \exp \left[ir \sqrt{\frac{4\pi K_\rho K_\sigma}{\cos^2 \alpha K_\rho + \sin^2 \alpha K_\sigma}} \theta'_1(0) \right] \quad (\text{D.19})$$

of dimension [32]:

$$d_{1n} = \frac{2r^2 K_\rho K_\sigma}{\cos^2 \alpha K_\rho + \sin^2 \alpha K_\sigma}. \quad (\text{D.20})$$

As above, from Eq. (18),

$$d_{1n} = 1/d_1 \quad (\text{D.21})$$

where d_1 is the dimension of t_1 , the coupling of the Majorana mode to channel 1. Thus, whenever the coupling to the Majorana mode is relevant, so that a flow may occur to the $A \otimes N$ fixed point, normal backscattering in channel 1 is irrelevant.

Now consider the coupling of channel 2 to the Majorana mode, from Eq. (15):

$$H_{b2} = 2t_2\tau_0^{-1+d_2}\gamma\Gamma_2 \cos[\sqrt{\pi}\phi_2(0)]. \quad (\text{D.22})$$

Making the Schrieffer-Wolff transformation discussed above we obtain:

$$\delta H \propto \frac{t_2^2}{t_1} \cos \left[r \sqrt{\frac{4\pi}{\cos^2 \alpha K_\rho + \sin^2 \alpha K_\sigma}} \phi'_2(0) \right] \quad (\text{D.23})$$

which has scaling dimension:

$$d_{2,A \otimes N} = \frac{2r^2}{\cos^2 \alpha K_\rho + \sin^2 \alpha K_\sigma}. \quad (\text{D.24})$$

This has the value $d_{2,A \otimes N} = 2$ for free fermions, $\alpha = 0$, $K_\rho/r^2 = 1$ and we generally expect it to increase with repulsive interactions, thus being strongly irrelevant.

Finally, we can consider processes where the number of electrons in channel 1 and 2 simultaneously change by ± 1 .

$$\begin{aligned} H_{12} &\propto \psi_1(0)\psi_2(0) \propto \cos[\sqrt{\pi}\theta_1(0)] \exp[i\sqrt{\pi}\phi_2(0)] \\ &\propto \cos \left[r \sqrt{\frac{\pi K_\rho K_\sigma}{\cos^2 \alpha K_\rho + \sin^2 \alpha K_\sigma}} \theta'_1(0) \right] \\ &\times \exp \left[ir \sqrt{\frac{\pi}{\cos^2 \alpha K_\rho + \sin^2 \alpha K_\sigma}} \phi'_2(0) \right] \end{aligned} \quad (\text{D.25})$$

of dimension

$$d_{12} = (1/4)(d_{1n} + d_{2,A \otimes N}) = \frac{r^2(1 + K_\rho K_\sigma)}{2[\cos^2 \alpha K_\rho + \sin^2 \alpha K_\sigma]}. \quad (\text{D.26})$$

This appears likely to be the most relevant operator at the $A \otimes N$ fixed point and may destabilize it in some cases as discussed above for the T -junction case. It is marginal in the $SU(2)$ symmetric case, $r = 1$, $\alpha = \pi/4$, $K_\sigma = 1$. This is to be expected since, as discussed in Sec. II, in the $SU(2)$ symmetric case there is a circle of rotated $A \otimes N$ fixed

points in which the linear combination of the ψ_i 's defined in Eq. (24) experiences perfect Andreev reflection and the orthogonal linear combination perfect normal reflection. Thus the $A \otimes N$, fixed point, whose stability we are studying, is merely one point on this circle and the exactly marginal operator drives the system along the line. Of course, setting $\alpha \rightarrow 0$, $K_\sigma \rightarrow K_1/r^2$, $K_\rho \rightarrow K_2 r^2$ we recover the result of Eq. (D.9). As discussed below Eq. (D.9) and in Fig. (D1), these processes can become relevant, destabilizing the $A \otimes N$ fixed point even when $K_1 < K_2 < 1$. Similarly the $A \otimes N$ fixed point may be unstable for coupled channels when the self-interactions in channel 1 are more strongly repulsive than in channel 2.

Appendix E. Stability of the non-trivial critical point

In Sec. II we showed that, for $0 < \epsilon_i \ll 1$, there was a separatrix in the phase diagram, at $t_1 = t_2$ in the case $\epsilon_1 = \epsilon_2$, separating the $A \otimes N$ and $N \otimes A$ phases. The RG flow along this separatrix was found in Sec. II to be to a non-trivial critical point. In this Appendix we wish to argue that this likely remains true for all Luttinger parameters such that both $A \otimes N$ and $N \otimes A$ fixed points are stable. This parameter range was calculated in Appendix D. For the T -junction (decoupled channels) it is the region obeying the 4 inequalities:

$$\begin{aligned} K_1 &> 1/2 \\ K_2 &> 1/2 \\ K_1 + \frac{1}{K_2} &> 2 \\ K_2 + \frac{1}{K_1} &> 2. \end{aligned} \tag{E.1}$$

This region is labelled number 1 in Fig. (D1a).

One way of arguing for this is based on “what else could happen”? When both $A \otimes N$ and $N \otimes A$ fixed points are stable, something must separate these two phases. One logical possibility might seem to be an $A \otimes A$ fixed point. We argue here that this is not possible. A quick way of seeing this is to consider, as in Appendix D, processes that change the number of electrons in both channels by ± 1 . Imposing $A \otimes A$ boundary conditions, this perturbation bosonizes as:

$$\delta H \propto \cos[\sqrt{\pi}\theta_1(0)] \cos[\sqrt{\pi}\theta_2(0)]. \tag{E.2}$$

For decoupled channels this has dimensions $d = (K_1 + K_2)/2$ and is thus relevant for repulsive interactions. In the general case, we can write:

$$\begin{aligned} \delta H &\propto \cos[\sqrt{\pi}(\theta_1 + \theta_2)] + \cos[\sqrt{\pi}(\theta_1 - \theta_2)] \\ &= \sum_{\pm} \cos[(r \cos \alpha \mp r^{-1} \sin \alpha)\theta_\sigma + (r \sin \alpha \pm r^{-1} \cos \alpha)\theta_\rho]. \end{aligned} \tag{E.3}$$

These two terms have dimensions:

$$d_{\pm} = \frac{1}{2}[(r^2 \cos^2 \alpha + r^{-2} \sin^2 \alpha \mp \sin 2\alpha)K_\sigma + (r^2 \sin^2 \alpha + r^{-2} \cos^2 \alpha \pm \sin 2\alpha)K_\rho]. \tag{E.4}$$

For the case of equivalent channels, $r = 1$, $\alpha = \pi/4$, these reduce to $d_+ = K_\sigma$, $d_- = K_\rho$. In this case, this interaction is relevant whenever K_ρ or $K_\sigma < 1$. This is consistent with our result in Appendix G that the impurity ground state degeneracy, g , is larger for the $A \otimes A$ fixed point than for the $N \otimes N$ fixed point at $t_i = 0$. The “ g -theorem” then implies that renormalization from $N \otimes N$ to $A \otimes A$ fixed points is impossible.

The careful reader might wonder whether the interaction of Eq. (E.2) is really allowed at the $A \otimes A$ fixed point given the delicate entanglement of the Majorana mode with both channels at such a fixed point. In Appendix D we found that a particular perturbation of another fixed point disrupted such an entangled state, driving the system into a high energy state and necessitating a Schrieffer-Wolff transformation resulting in a higher dimension operator. Does this also happen here? To check this point, it is useful to consider a rather contrived tight-binding model which really is described at low energies by an $A \otimes A$ fixed point. We note that this *does not* correspond to simply taking large $t_1 = t_2 \equiv t$ in the Hamiltonian of Eq. (C.1). Setting $J_i = V_i = U = 0$ in Eq. (C.1) gives the “strong coupling Hamiltonian”

$$H_{sc} = -t(c_0^\dagger + c_0)(c_1^\dagger - c_1 + c_{-1}^\dagger - c_{-1})/2. \quad (\text{E.5})$$

Expanding in Majorana fermions:

$$\begin{aligned} c_0 &\equiv (\gamma + i\gamma')/2 \\ c_j &\equiv (\gamma'_j + i\gamma_j)/2, \quad (j = \pm 1), \end{aligned} \quad (\text{E.6})$$

H_{sc} can be rewritten:

$$H_{sc} = it\gamma(\gamma_1 + \gamma_{-1})/2. \quad (\text{E.7})$$

The appropriate Dirac operator, annihilating the ground state of H_{sc} is:

$$\psi_0 \equiv [\gamma + i(\gamma_1 + \gamma_{-1})/\sqrt{2}]/2. \quad (\text{E.8})$$

However, to check whether or not large t really corresponds to an $A \otimes A$ fixed point we must consider the effect of turning on the J_i , V_i and U interactions. To keep things as simple as possible, we consider only the non-interacting case with $V_i = U = 0$. We also set $J_1 = J_2$. The hopping terms from sites 1 to 2 and (-1) to (-2) are:

$$\begin{aligned} H_{12} = & -J(c_1^\dagger c_2 + c_{-1}^\dagger c_{-2} + h.c.) = -J[\gamma'_1(c_2 - c_2^\dagger) - i\gamma_1(c_2 + c_2^\dagger) \\ & + \gamma'_{-1}(c_{-2} - c_{-2}^\dagger) - i\gamma_{-1}(c_{-2} + c_{-2}^\dagger)]/2. \end{aligned} \quad (\text{E.9})$$

The terms in H_{12} involving the γ'_j operators are harmless but the terms involving the γ_j operators disrupt the localized state of the putative $A \otimes A$ fixed point. In order to study the stability of this fixed point we temporarily allow these couplings to be different, changing H_{12} to:

$$H_{12} = -J[\gamma'_1(c_2 - c_2^\dagger) + \gamma'_{-1}(c_{-2} - c_{-2}^\dagger)]/2 + i\tilde{J}[\gamma_1(c_2 + c_2^\dagger) + \gamma_{-1}(c_{-2} + c_{-2}^\dagger)]/2. \quad (\text{E.10})$$

If we now set $\tilde{J} = 0$, but include the full J terms between all other pairs of sites, we indeed obtain a model which we expect to renormalize, at low energies, to an $A \otimes A$ fixed point. The Majorana mode γ'_1 entangles with the Dirac fermions on sites 2, 3, $\dots \infty$

to produce the analogue of the perfect Andreev scattering fixed point and likewise the Majorana mode γ'_{-1} entangles with the Dirac fermions on sites $-2, -3, \dots -\infty$. All of this can happen without disrupting the entanglement between the γ , γ_1 and γ_{-1} Majorana modes that occurs in the ground state of H_{sc} . The resulting ground states are 4-fold degenerate corresponding to occupancy zero or one for the two local modes: one constructed from γ'_1 and the chain on the right and the other constructed from γ'_{-1} and the chain on the left. As in Sec. II we may bosonize these two semi-infinite chains, introduce Klein factors Γ_1 and Γ_2 , and construct the local Dirac operators $(\gamma'_1 + i\Gamma_1)/2$ and $(\gamma'_{-1} + i\Gamma_2)/2$. But now consider the effect of turning on a small \tilde{J} . Acting to first order in \tilde{J} drives the system into a high energy state of H_{sc} . However, at second order in \tilde{J} the system can return to the ground state of H_{sc} and we develop, via a Schrieffer-Wolff type transformation, a perturbation of the $A \otimes A$ fixed point of the form:

$$\delta H \propto \frac{\tilde{J}^2}{t} (c_2 + c_2^\dagger)(c_{-2} + c_{-2}^\dagger). \quad (\text{E.11})$$

This is precisely the relevant perturbation of Eq. (E.2), that changes the number of electrons in channels 1 and 2 by ± 1 . In this non-interacting example, we expect it to drive the system from the unstable $A \otimes A$ fixed point to the rotated $A \otimes N$ fixed point discussed in Sec. II. This argument goes through the same way for general J_i , V_i and U . We could again artificially separate V into terms that do and do not disrupt the Majorana entanglement in the $A \otimes A$ ground state. The relevant perturbation now also contains a term $\propto (\tilde{V})^2/t$. In this case, we expect the relevant perturbation would drive the system to the nontrivial critical point (or else the $A \otimes N$ or $N \otimes A$ critical points off the separatrix).

The above arguments imply that, even along the separatrix, there is no stable $A \otimes A$ fixed point to compete with our non-trivial one. It is thus difficult for us to imagine how it could not exist in the phase diagram. We provide further evidence for this in Appendix G, where we calculate the impurity entropies at the various fixed points and invoke the “g-theorem”.

There is however, one interesting possibility that may warrant numerical investigation. Could our nontrivial critical point become *completely* stable under arbitrary small variations of the t_i ’s and other parameters for some range of bulk interaction parameters? In this case the t_1 - t_2 plane would divide up into regions of finite area attracted to the $A \otimes N$, $N \otimes A$ and nontrivial critical points. Thus assuming continuous phase transitions between these phases, there would then need to be two other (equivalent) fixed points, unstable in one direction, on these separatrices, as sketched in Fig. (E1).

Appendix F. Uniform wire coupled to superconductor far from its end points

So far, the T -junction we have considered consists of two quantum wires, end-coupled to the topological superconductor, as sketched in Fig.1. In this Appendix we consider

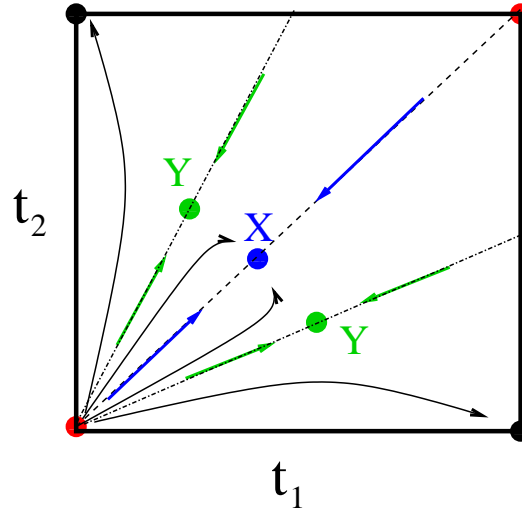


Figure E1. Qualitative sketch of the putative phase diagram for a range of Luttinger parameters where the nontrivial critical point, X , might be stable. In this case, two other fixed points, Y , exist on the two separatrixes.

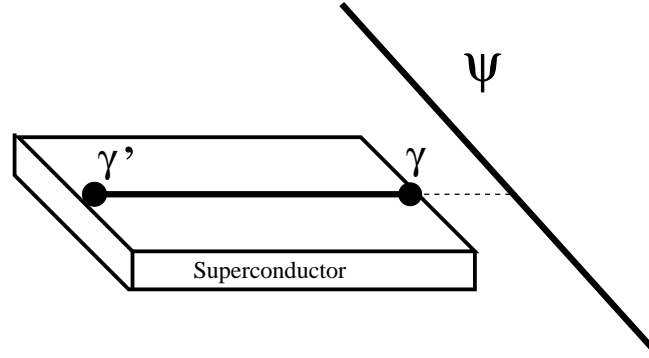


Figure F1. A sketch of the uniform chain coupled to the topological superconductor far from its endpoints

the opposite extreme of a single channel uniform quantum wire “centre-coupled” far from its endpoints to the topological superconductor, as sketched in Fig. (F1). Despite the extreme difference in the underlying model, we obtain the same phase diagram. In general, at low energies, the wire breaks up into two sections at the junction with one side coupling strongly to the Majorana mode and exhibiting perfect Andreev reflection while the other side decouples, exhibiting perfect normal reflection. Or, if a suitable parity symmetry is respected, the NTCP occurs.

We begin by considering the low energy effective Hamiltonian:

$$\begin{aligned}
 H_0 &= i \int_{-\infty}^{\infty} dx [\psi_R^\dagger \partial_x \psi_R - \psi_L^\dagger \partial_x \psi_L] \\
 H_{\text{int}} &= V \int_{-\infty}^{\infty} dx \psi_R^\dagger \psi_R \psi_L^\dagger \psi_L \\
 H_b &= \gamma [t_L(\psi_L^\dagger(0) - \psi_L(0)) + t_R(\psi_R^\dagger(0) - \psi_R(0))].
 \end{aligned} \tag{F.1}$$

Bosonizing we obtain the bulk Hamiltonian

$$H = \frac{1}{2}u \int_0^\infty dx \left[K \left(\frac{\partial \phi}{\partial x} \right)^2 + K^{-1} \left(\frac{\partial \theta}{\partial x} \right)^2 \right]. \quad (\text{F.2})$$

The “boundary” Hamiltonian is:

$$H_b = i\gamma \{ t_L \cos[\sqrt{\pi}(\phi(0) + \theta(0))] + t_R \cos[\sqrt{\pi}(\phi(0) - \theta(0))] \}. \quad (\text{F.3})$$

Note that no boundary conditions are imposed on ϕ or θ in this case; we start with a continuous translationally invariant chain at $t_L = t_R = 0$. The boundary interactions both have dimension:

$$d_b = \frac{1}{4} \left(K + \frac{1}{K} \right) \quad (\text{F.4})$$

1/2 at the free fermion point, $K = 1$ and increasing when K increases or decreases. They become marginal at $K_c = 2 \pm \sqrt{3} \approx 3.73, .268$.

We now calculate the cubic term in the β functions at the marginal point. (Only the one at $K = .268 \dots$ is likely to be of physical interest.) We first change variables to $\bar{\phi} \equiv \sqrt{K}\phi$, $\bar{\theta} \equiv \theta/\sqrt{K}$ as in Appendix D. We then change variables to $\phi_{L/R}$ defined by:

$$\begin{aligned} \bar{\phi} &\equiv \phi_L + \phi_R \\ \bar{\theta} &\equiv \phi_L - \phi_R. \end{aligned} \quad (\text{F.5})$$

Then:

$$\begin{aligned} &\psi_L^\dagger(\tau_1) \psi_L(\tau_2) \psi_R(\tau_3) \propto \\ &\exp \left\{ i\sqrt{\pi} \left[(1/\sqrt{K} + \sqrt{K})[\phi_L(\tau_2) - \phi_L(\tau_1)] + (1/\sqrt{K} - \sqrt{K})\phi_L(\tau_3) \right] \right\} \\ &\cdot \exp \left\{ i\sqrt{\pi} \left[(1/\sqrt{K} - \sqrt{K})[\phi_R(\tau_2) - \phi_R(\tau_1)] + (1/\sqrt{K} + \sqrt{K})\phi_R(\tau_3) \right] \right\} \end{aligned} \quad (\text{F.6})$$

This gives an OPE:

$$\begin{aligned} \mathcal{T} &< \psi_L^\dagger(\tau_1) \psi_L(\tau_2) \psi_R(\tau_3) > \\ &\rightarrow \epsilon(\tau_1 - \tau_2) \left| \frac{1}{\tau_{12}} \right|^{[(1/\sqrt{K} + \sqrt{K})^2 + (1/\sqrt{K} - \sqrt{K})^2]/4} \cdot \left| \frac{\tau_{23}}{\tau_{13}} \right|^{(1/\sqrt{K} + \sqrt{K})(1/\sqrt{K} - \sqrt{K})/2} \psi_R(\tau_3) \\ &= \epsilon(\tau_1 - \tau_2) \left(\frac{1}{\tau_{12}} \right)^2 \left| \frac{\tau_{23}}{\tau_{13}} \right|^{\sqrt{3}} \psi_R(\tau_3). \end{aligned} \quad (\text{F.7})$$

Here we used $K = 2 - \sqrt{3}$. Including the Majorana mode OPE of Eq. (B.5), this gives Eq. (B.33) with $\nu = \sqrt{3} > 1$. As we see from Fig. (B1), $\mathcal{F}(\nu)$ is negative, for $\nu > 1$, with $\mathcal{F}(\sqrt{3}) \approx -20$. So, in this case there is no nontrivial critical point for $\epsilon > 0$; instead the flow is towards infinite coupling for any bare couplings which are both non-zero. Furthermore, the negative \mathcal{F} drives the couplings towards each other, rather than apart, as the floating cut-off, D , is reduced, as illustrated in Fig. (F2). This might suggest a flow towards the NTCP, but this requires further substantiation. Note that, if we had instead found that $t_R \rightarrow 0$ and t_L grew large under renormalization this would suggest very exotic behaviour indeed, with the left-moving chiral mode having

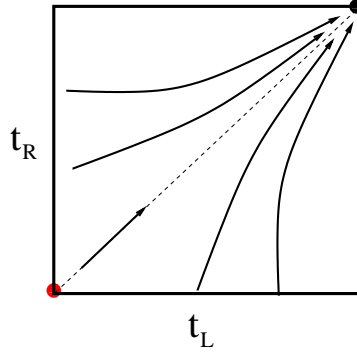


Figure F2. RG flow of effective couplings for $\mathcal{F} < 0$.

perfect Andreev transmission and the right-moving chiral mode having perfect normal transmission. However, due to the fact that $\nu > 1$, this *is not* what we are finding.

To test our hypothesized flow to the NTCP, it is very convenient to consider a tight-binding model whose continuum limit gives the Hamiltonian of Eq. (F.1). This is represented in Fig. (F3). The uniform chain has Hamiltonian:

$$H_0 + H_{\text{int}} = \sum_{j=-\infty}^{\infty} [-J(c_j^\dagger c_{j+1} + h.c.) + V n_j n_{j+1}]. \quad (\text{F.8})$$

The topological superconductor is represented by the impurity site, with annihilation operator $d = (\gamma + i\gamma')/2$ and impurity coupling:

$$H_b = t\gamma(c_0 - c_0^\dagger). \quad (\text{F.9})$$

Using the low energy representation of the tight binding model operators

$$c_j \approx e^{ik_F j} \psi_R(j) + e^{-ik_F j} \psi_L(j) \quad (\text{F.10})$$

establishes the low energy correspondence with the Hamiltonian of Eq. (F.1) in the case $t_L = t_R = t$. Since the perturbative RG analysis suggests that t renormalizes to large values, we consider the $t \rightarrow \infty$ limit of the tight-binding model. Writing:

$$c_0 = (\gamma_0 + i\eta_0)/2, \quad (\text{F.11})$$

we see that, in the $t \rightarrow \infty$ limit, η_0 combines with γ to form a local Dirac operator:

$$\psi_0 = (\gamma + i\eta_0)/2 \quad (\text{F.12})$$

which is empty in the ground state. In this limit, to avoid driving the system into a high energy state, the hopping term between sites 0 and ± 1 , is projected to:

$$-Jc_0^\dagger(c_1 + c_{-1}) + h.c. \rightarrow -J\gamma_0(c_1 + c_{-1}) + h.c. \quad (\text{F.13})$$

Up to a phase redefinition, this is precisely the tight-binding representation of our standard 2-channel model, with the sites at $j < 0$ and $j > 0$ corresponding to the two channels, introduced in Appendix C. Bosonizing all fermion operators except γ and c_0 , with open boundary conditions at $x = 0$, gives

$$H_b = it\gamma\eta_0 + iJ\gamma_0\{\Gamma_1 \cos[\sqrt{\pi}\phi_1(0)] + \Gamma_2 \cos[\sqrt{\pi}\phi_2(0)]\}. \quad (\text{F.14})$$

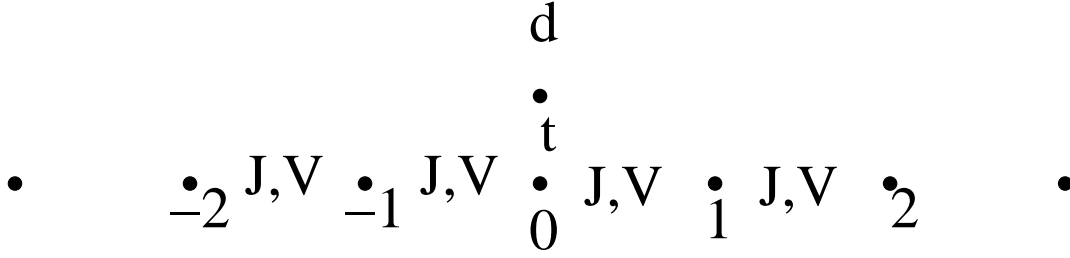


Figure F3. Tight-binding model of topological superconductor coupled far from the ends of a single channel quantum wire.

As established in Sec. II, Appendix B and Appendix E, this model renormalizes to the NTCP, confirming our conjecture based on naive extrapolation of the RG equations for the centre-coupled model. It is also interesting to analyze a tight-binding model which gives $t_L \neq t_R$. This is:

$$H_b = \gamma[t c_0 - it'(c_1 - c_{-1})] + h.c.] \quad (\text{F.15})$$

Using Eq. (F.10) we see that this gives, at low energies, our continuum model of Eq. (F.1) with

$$t_{L/R} = t \pm 2t' \sin k_F. \quad (\text{F.16})$$

Now the bosonized form is:

$$\begin{aligned} H_b = & it\gamma\eta_0 + iJ\gamma_0\{\Gamma_1 \cos[\sqrt{\pi}\phi_1(0)] + \Gamma_2 \cos[\sqrt{\pi}\phi_2(0)]\} \\ & + 2it'\eta_0\{\Gamma_1 \sin[\sqrt{\pi}\phi_1(0)] - \Gamma_2 \sin[\sqrt{\pi}\phi_2(0)]\}. \end{aligned} \quad (\text{F.17})$$

Again assuming t renormalizes to large values, we see that the t' term drives the system into a high energy state, due to the factor of η_0 . Performing a Schrieffer-Wolff transformation, the perturbation due to t' becomes:

$$\begin{aligned} H'_b \propto & \frac{(t')^2}{t} \{\Gamma_1 \sin[\sqrt{\pi}\phi_1(0)] - \Gamma_2 \sin[\sqrt{\pi}\phi_2(0)]\}^2 \\ = & \frac{(t')^2}{t} \{\sin^2[\sqrt{\pi}\phi_1(0)] + \sin^2[\sqrt{\pi}\phi_2(0)]\} \end{aligned} \quad (\text{F.18})$$

where $\{\Gamma_i, \Gamma_j\} = \delta_{ij}$ was used in the last step. This has dimension $2/K$ and is irrelevant for the range of physical interest, $K < 1$. This confirms our conjecture that the model renormalizes to the NTCP even when $t_L \neq t_R$.

We might enquire as to whether there is a symmetry protecting the non-trivial critical point in this model. Basically, coupling more strongly to left or right *movers* does not correspond to coupling more strongly to left or right *sides* and so, does not lead to a flow from the NTCP to the $A \otimes N$ or $N \otimes A$ fixed point where the Majorana mode couples strongly to the left or right side of the system. The operative symmetry is parity \times time-reversal, PT. This is an anti-unitary operator which complex conjugates c-numbers and takes:

$$\psi_L(x) \rightarrow \psi_L(-x), \quad \psi_R(x) \rightarrow \psi_R(-x), \quad \gamma \rightarrow \gamma \quad (\text{F.19})$$

in the continuum model and:

$$c_j \rightarrow c_{-j} \quad (\text{F.20})$$

in the lattice model. This is readily seen to be a symmetry of the Hamiltonian, in continuum and tight-binding forms, for all t and t' . Time reversal acts on the components of the conductance tensor, defined in Sec. III as $G_{ij} \rightarrow G_{ji}$. On the other hand, parity takes $G_{01} \rightarrow G_{02}$ and $G_{10} \rightarrow G_{20}$. Therefore PT takes $G_{01} \rightarrow G_{20}$. This is a symmetry of G_{ij} at the NTCP, Eq. (42), in the parity symmetric case where the G_{jc} defined in Eq. (40) are equal. However, it is *not* a symmetry of G_{ij} at the $A \otimes N$ critical point, Eq. (46). Thus, PT symmetry prevents a flow to $A \otimes N$, stabilizing the NTCP. When PT symmetry is broken, a flow *does* occur to the $A \otimes N$ or $N \otimes A$ critical point. In the continuum model, PT symmetry is broken by:

$$\delta H = iV(\psi_L^\dagger \psi_R - h.c.) \quad (\text{F.21})$$

which is relevant at the $t_L = t_R = 0$ fixed point, but less relevant than $t_{L/R}$. This interaction arises in the continuum limit from the perturbation in the lattice model:

$$\delta H = J'c_0^\dagger(c_1 - c_{-1}) + h.c. \quad (\text{F.22})$$

giving $V = 2J' \sin k_F$. Bosonizing Eq. (F.22) and projecting c_0 gives:

$$\delta H = iJ'\eta_0\{\Gamma_1 \cos[\sqrt{\pi}\phi_1(0)] - \Gamma_2 \cos[\sqrt{\pi}\phi_2(0)]\} \quad (\text{F.23})$$

which, as we know from Sec. II, leads to an RG flow to $A \otimes N$ or $N \otimes A$.

To conclude this Appendix, even the very different centre-coupled model exhibits the same phase diagram with stable $A \otimes N$ and $N \otimes A$ critical points and a NTCP which is stabilized by an appropriate parity symmetry, providing further evidence for the universality of our proposed phase diagram.

Appendix G. Impurity Entropy

Critical points of quantum impurity models with boundary conformal invariance can be characterized by a universal zero temperature impurity entropy [33, 34], whose exponential is denoted by g , the “ground state degeneracy”. This thermodynamic impurity entropy is experimentally measurable for some systems such as dilute magnetic impurities in metals. Furthermore, the same universal quantity, $\ln g$, appears [36] as an impurity contribution to the ground state entanglement entropy, a convenient quantity for characterizing phases of one dimensional models via DMRG methods. g is known to always decrease under RG flows [33, 34, 35]. Thus determining g at various fixed points can put constraints on possible phase diagrams. In this section we calculate g for the various stable and unstable fixed points discussed in this paper.

Conformally invariant critical points of quantum impurity models are characterized by conformally invariant boundary conditions (CIBC's). We label these by an integer, A with the corresponding ground state degeneracy g_A . Imposing boundary conditions A and B at the two ends of a strip of length ℓ determines a finite size spectrum of energies

$E^n = x_{AB}^n u / \ell$ for some dimensionless universal real numbers x_{AB}^n . (u is the velocity.) The corresponding partition function, at temperature T , is:

$$Z_{AB}[u/(\ell T)] = \sum_n \exp[-x_{AB}^n (u/\ell T)]. \quad (\text{G.1})$$

(Non-universal terms in the ground state energy, of $O(\ell)$ and $O(1)$ are dropped from Z .) It is important to note that $Z_{AB}[u/(\ell T)]$ is a universal function of the dimensionless ratio $u/(\ell T)$ only. In the limit $u/(\ell T) \rightarrow 0$, it has the asymptotic form:

$$Z_{AB}[u/(\ell T)] \rightarrow g_A g_B e^{\pi \ell T c / (6u)}. \quad (\text{G.2})$$

Here c is the ‘‘conformal anomaly’’ parameter which characterizes the bulk conformal field theory and is independent of the boundary conditions A and B . For the model we are considering, $c = 2$. The exponential factor in Eq. (G.2) gives a term in the free energy quadratic in temperature and hence the universal low temperature *bulk* entropy [37]:

$$S_{\text{bulk}} = \pi \ell T c / (3u) \quad (\text{G.3})$$

independent of the boundary conditions. In addition there is an *impurity* entropy:

$$S_{\text{imp}} = \ln g_A + \ln g_B \quad (\text{G.4})$$

which is independent of l and T and is a sum of contributions from both boundaries of the system.

Note that the order of limits is important here. We take $\ell \rightarrow \infty$ first, then take $T \rightarrow 0$. In this limit, many non-universal contributions to the partition function, associated with irrelevant operators, become negligible and the asymptotic form of Eq. (G.2) applies. An additional ground state energy factor:

$$Z_{AB} \rightarrow Z_{AB} \exp[-e_0 \ell / T - e_1 / T] \quad (\text{G.5})$$

will generally be present. However, the boundary-dependent term in the ground state energy, e_1 , can easily be distinguished from the impurity entropy by its temperature-dependence. The ground state degeneracy can also be defined by this method for a system with 2 or more channels of decoupled gapless bulk excitations with different velocities, u_j . Since we are only concerned with critical phenomena at the boundary here, we can formally rescale the lengths differently for each channel to make the u_j equal. Without rescaling, Eq. (G.2) still applies in the more general form:

$$Z_{AB}[u/(\ell T)] \rightarrow g_A g_B \exp[\pi \ell T \sum_j c_j / (6u_j)]. \quad (\text{G.6})$$

where c_j is the conformal anomaly for the bulk sector with velocity u_j . In our case we have 2 channels of free bosons, so $c_1 = c_2 = 1$.

Thus a straightforward method to determine g_A for some CIBC A , is to first calculate the finite size spectrum with A -type boundary conditions at both ends of a system of length l . The corresponding partition function, $Z_{AA} \propto g_A^2$ in the appropriate limit. We will follow this procedure, restricting our Luttinger liquid channels to have length ℓ and coupling them to topological superconductors at both ends with identical

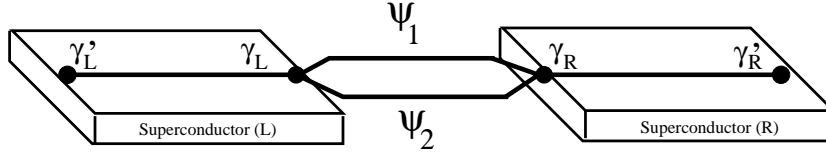


Figure G1. A finite system of 2 channels coupled to topological superconductors at both ends.

couplings, as sketched in Fig. (G1). To get a well-defined value for g_A , we are careful to include the other Majorana mode, γ' localized at the other end of the superconductor, far from the junction.

Appendix G.1. $N \otimes N$ fixed point

We begin with the limit $t_i = 0$ where the superconductor is decoupled from the two Luttinger liquid channels which obey “open”, that is “perfect normal reflection” boundary conditions at both ends: $\psi_L = \psi_R$. From Eq. (9) this corresponds to:

$$\theta_i(0) = \theta_i(\ell) = 0, \pmod{\sqrt{\pi}}. \quad (\text{G.7})$$

We may also derive these boundary conditions by considering a large normal scattering boundary interaction:

$$H_{bN} = -t_N \sum_j [\psi_{Li}^\dagger \psi_{Ri} + h.c.] = -t_N \sum_j \cos[2\sqrt{\pi}\theta_j]. \quad (\text{G.8})$$

Requiring θ_j to be at the minimum of H_{bN} at $x = 0$ and ℓ gives Eq. (G.7).

Let us begin with the simplest case of decoupled channels, the T-junction. Then the fields θ_i and ϕ_i have the mode expansions:

$$\begin{aligned} \theta_j(x) &= \frac{\sqrt{\pi}x}{\ell} p_j + i \sum_{n=1}^{\infty} \sqrt{\frac{K_j}{\pi n}} \sin\left[\frac{\pi n x}{\ell}\right] [\alpha_{n,j} - \alpha_{n,j}^\dagger] \\ \phi_j(x) &= \phi_j^0 + \sum_{n=1}^{\infty} \frac{1}{\sqrt{K_j \pi n}} \cos\left[\frac{\pi n x}{\ell}\right] [\alpha_{n,j} + \alpha_{n,j}^\dagger]. \end{aligned} \quad (\text{G.9})$$

Here the p_j are integers, the ϕ_j^0 's are constants and the $\alpha_{n,j}$ are harmonic oscillator annihilation operators. In deriving Eq. (G.9) we have used the fact that when $\theta_j(x)$ obeys Dirichlet boundary conditions, $\phi_j(x)$ must obey Neumann boundary conditions, $d\phi_j/dx(0) = d\phi_j/dx(\ell) = 0$. Letting $m_{n,j} = 0, 1, 2, \dots \infty$ label the eigenvalues of $\alpha_{n,j}^\dagger \alpha_{n,j}$, the finite size spectrum becomes:

$$E[p_j, m_{n,j}] = \sum_{j=1}^2 \frac{\pi u_j}{\ell} \left[\frac{p_j^2}{2K_j} + \sum_{n=1}^{\infty} m_{n,j} n \right]. \quad (\text{G.10})$$

This gives the partition function:

$$Z_{N \otimes N, N \otimes N} = 4 \prod_{j=1}^2 \left\{ \left[\sum_{p=-\infty}^{\infty} \exp[-\pi u_j p^2 / (2\ell T K_j)] \right] \cdot \prod_{n=1}^{\infty} \{1 - \exp[-\pi u_j n / (\ell T)]\}^{-1} \right\} \quad (\text{G.11})$$

The prefactor of 4 was inserted to account for the zero modes in the superconductor on the left and right side of the wires. To extract g_N , we must take the limit $u_j/(\ell T) \rightarrow 0$. The second factor in Eq. (G.11) is proportional to the Dedekind η -function and has the asymptote:

$$\prod_{n=1}^{\infty} \{1 - \exp[-\pi u_j n/(\ell T)]\}^{-1} \rightarrow \sqrt{\frac{u_j}{2\ell T}} \exp[\pi \ell T/(6u_j)]. \quad (\text{G.12})$$

The sum in Eq. (G.11) can be approximated, when $u_j/\ell T \ll 1$ by an integral:

$$\sum_{p=-\infty}^{\infty} \exp[-\pi u_j p^2/(2\ell T K_j)] \approx \int_{-\infty}^{\infty} dp \exp[-\pi u_j p^2/(2\ell T K_j)] = \sqrt{\frac{2\ell T K_j}{u_j}}. \quad (\text{G.13})$$

Thus:

$$Z_{N \otimes N, N \otimes N} \rightarrow 4 \prod_{j=1}^2 \sqrt{K_j} \exp[\pi T/(6u_j)]. \quad (\text{G.14})$$

This has the expected form of Eq. (G.6) and allows us to extract the ground state degeneracy with $N \otimes N$ boundary conditions, in this simple case [38]:

$$g_{N \otimes N} = 2(K_1 K_2)^{1/4}. \quad (\text{G.15})$$

Now consider the general $N \otimes N$ case, with arbitrary bulk parameters, as defined in Sec. II. We then have:

$$\begin{aligned} \cos \alpha \theta_{\sigma}(\ell) + \sin \alpha \theta_{\rho}(\ell) &= \sqrt{\pi} p_1/r \\ -\sin \alpha \theta_{\sigma}(\ell) + \cos \alpha \theta_{\rho}(\ell) &= \sqrt{\pi} p_2/r \end{aligned} \quad (\text{G.16})$$

for arbitrary integers p_1 and p_2 . Thus the mode expansions are modified to:

$$\begin{aligned} \theta_{\sigma}(x) &= \frac{\sqrt{\pi} x}{\ell} (\cos \alpha p_1/r - \sin \alpha p_2/r) + i \sum_{n=1}^{\infty} \sqrt{\frac{K_{\sigma}}{\pi n}} \sin \left[\frac{\pi n x}{\ell} \right] [\alpha_{n,\sigma} - \alpha_{n,\sigma}^{\dagger}] \\ \theta_{\rho}(x) &= \frac{\sqrt{\pi} x}{\ell} (\sin \alpha p_1/r + \cos \alpha p_2/r) + i \sum_{n=1}^{\infty} \sqrt{\frac{K_{\rho}}{\pi n}} \sin \left[\frac{\pi n x}{\ell} \right] [\alpha_{n,\rho} - \alpha_{n,\rho}^{\dagger}] \end{aligned} \quad (\text{G.17})$$

and the finite size spectrum becomes:

$$\begin{aligned} E[p_j, m_{n,\lambda}] &= \frac{\pi}{\ell} \left[\frac{u_{\sigma}}{2K_{\sigma}} (\cos \alpha p_1/r - \sin \alpha p_2/r)^2 + \frac{u_{\rho}}{2K_{\rho}} (\sin \alpha p_1/r + \cos \alpha p_2/r)^2 \right. \\ &\quad \left. + \sum_{\lambda} u_{\lambda} \sum_{n=1}^{\infty} m_{n,\lambda} n \right]. \end{aligned} \quad (\text{G.18})$$

We may evaluate $Z_{N \otimes N, N \otimes N}$ at $u_i/(\ell T) \rightarrow 0$ as before. The needed Gaussian integral

$$\begin{aligned} &\int_{-\infty}^{\infty} dp_1 dp_2 \exp \left\{ -\frac{\pi}{2\ell} \left[\frac{u_{\sigma}}{K_{\sigma}} (\cos \alpha p_1/r - \sin \alpha p_2/r)^2 + \frac{u_{\rho}}{K_{\rho}} (\sin \alpha p_1/r + \cos \alpha p_2/r)^2 \right] \right\} \\ &= 2\ell T \sqrt{\frac{K_{\sigma} K_{\rho}}{u_{\sigma} u_{\rho}}}, \end{aligned} \quad (\text{G.19})$$

is independent of α and r , as can be seen by making the rotation of the vector of integration co-ordinates (p_1, p_2) , $\vec{p}' = M^T \vec{p}$, where the matrix M is defined in Eq. (A.7),

before performing the integration. (We use the fact that $\text{Det } M = 1$.) Thus, our general result is:

$$g_{N \otimes N} = 2(K_\rho K_\sigma)^{1/4}, \quad (\text{G.20})$$

independent of α .

Appendix G.2. $A \otimes N$ fixed point

Now suppose we have a relevant boundary interaction Eq. (15) in channel 1 but channel 2 still obeys normal boundary conditions.

Let us begin with the simpler T-junction case of decoupled channels. Then $Z_{A \otimes N, A \otimes N}$ factorizes into contributions from each channel. The normal channel 2 contributes a factor of $K_2^{1/2}$, as above. To calculate the partition function for channel 1 we write the sum of boundary Hamiltonians at each boundary as:

$$H_b = 2ti\{\gamma_L \Gamma_1 \cos[\sqrt{\pi}\phi(0)] + \gamma_R \Gamma_1 \cos[\sqrt{\pi}\phi(\ell)]\} \quad (\text{G.21})$$

Here $\gamma_{L/R}$ are the Majorana modes at the SN junctions at $x = 0$ and ℓ respectively and Γ_1 is the Klein factors corresponding to channel-1. t is assumed to be large. As discussed above, the A boundary conditions imply pinning of both $\phi(0)$ and $\phi(\ell)$ to integer multiples of $\sqrt{\pi}$. Then we have the mode expansion:

$$\phi_1(x) = \sqrt{\pi} \frac{mx}{\ell} + \dots \quad (\text{G.22})$$

for m an arbitrary integer. Accordingly, the 2 possible states of the superconductors correspond to $\frac{1}{\sqrt{2}}\{\gamma_L \Gamma_1 \cos[\sqrt{\pi}\phi(0)] + \gamma_R \Gamma_1 \cos[\sqrt{\pi}\phi(\ell)]\} = \pm 1$. As the system lies within the minimum energy state, there is a real fermion "left-over", corresponding to the combination of γ_L and γ_R "orthogonal" to $\frac{1}{\sqrt{2}}\{\gamma_L \Gamma_1 \cos[\sqrt{\pi}\phi(0)] + \gamma_R \Gamma_1 \cos[\sqrt{\pi}\phi(\ell)]\}$. Together with the Klein factor corresponding to channel-2, Γ_2 , this yields a degeneracy factor of 2, which, when calculating the partition function as above, for $\ell T \gg u_i$ now gives:

$$Z_{A \otimes N, A \otimes N} = 2\sqrt{K_2/K_1} \prod_j e^{\pi \ell T / (6u_j)}. \quad (\text{G.23})$$

Thus we obtain, for a single channel with Andreev boundary conditions:

$$g_A = \sqrt{2}/K_1^{1/4} \quad (\text{G.24})$$

and for the 2 channel case:

$$g_{A \otimes N} = \sqrt{2}(K_2/K_1)^{1/4}. \quad (\text{G.25})$$

Note that $g_{N \otimes N}/g_{A \otimes N} = \sqrt{2K_1}$, so the g -theorem implies the RG flow is from $N \otimes N$ to $A \otimes N$ fixed points for $K_1 > 1/2$, consistent with the RG scaling dimension of the boundary interactions discussed in Sec. II and Appendix D.

Now consider the general case of coupled channels. As discussed in Appendix A, the corresponding boundary conditions on the boson fields are most conveniently written

in terms of the rotated and rescaled fields ϕ'_i, θ'_i . Using Eq. (9) and Eq. (D.18) these conditions require:

$$\begin{aligned}\phi'_1(0) &= \phi'_1(\ell), \quad [\text{mod } r\sqrt{\pi K_\rho K_\sigma / (\cos^2 \alpha K_\rho + \sin^2 \alpha K_\sigma)}] \\ \theta'_2(0) &= \theta'_2(\ell), \quad [\text{mod } r\sqrt{\pi / (\cos^2 \alpha K_\rho + \sin^2 \alpha K_\sigma)}].\end{aligned}\tag{G.26}$$

Thus the mode expansions for the primed fields are:

$$\begin{aligned}\phi'_1(x) &= \sqrt{\frac{\pi K_\rho K_\sigma}{\cos^2 \alpha K_\rho + \sin^2 \alpha K_\sigma}} \frac{x}{l} p_{1r} + \dots \\ \theta'_2(x) &= \sqrt{\frac{\pi}{\cos^2 \alpha K_\rho + \sin^2 \alpha K_\sigma}} \frac{x}{l} p_{2r} + \dots\end{aligned}\tag{G.27}$$

Repeating the above calculation gives, in general:

$$g_{A \otimes N} = g_{A \otimes N} = \sqrt{2} \left\{ \frac{4K_\rho K_\sigma}{r^4 [\cos^2(\alpha) K_\sigma^2 + \sin^2(\alpha) K_\rho^2]} \right\}^{\frac{1}{4}}.\tag{G.28}$$

Combining this with Eq. (G.20) we have:

$$\left(\frac{g_{A \otimes N}}{g_{N \otimes N}} \right)^2 = \frac{1}{\sqrt{2} K_1} \left[1 - \frac{\tilde{U}^2}{u_1 u_2} \right]^{\frac{1}{4}} = 1/\sqrt{d_1}\tag{G.29}$$

where d_1 , given in Eq. (18), is the dimension of t_1 at the normal fixed point. Again we obtain consistency with the g -theorem: the flow from $N \otimes N$ to $A \otimes N$ fixed points only occurs when $d_1 < 1$ so that g decreases.

Appendix G.3. $A \otimes A$ fixed point

As discussed in Appendix E, by artificially tuning parameters we can reach an $A \otimes A$ fixed point, formally corresponding to $t_1 = t_2 \rightarrow \infty$. We argued in Appendix E that this is an unstable fixed point, renormalizing to the NTCP if the couplings are tuned to lie on the separatrix, and otherwise renormalizing to $A \otimes N$ or $N \otimes A$. It is interesting to calculate g at this unstable fixed point since this will help us to confirm its instability, once we invoke the g -theorem.

We first consider the T-junction (decoupled channels) and follow the approach of Appendix G.2. From Appendix E, we see that at the $A \otimes A$ fixed point each channel is coupled to a separate Majorana mode, γ'_1 and γ'_{-1} . The original Majorana mode γ is eliminated from the low energy effective Hamiltonian since it combines to make a gapped local Dirac mode defined in Eq. (E.8). Multiplying together the two g_A factors, from Eq. (G.24) would give $2/(K_1 K_2)^{1/4}$. However, we get an extra factor of 2 due to two other Majorana modes which both commute with the low energy effective Hamiltonian. These are $(\gamma_1 - \gamma_{-1})/\sqrt{2}$ and γ' . Here $\gamma_{\pm 1}$ are defined in (E.8) and γ' is the ever-present Majorana mode at the other end of the topological superconductor. We may construct a Dirac zero mode operator out of these and the corresponding state can be filled or empty, giving the extra factor of 2. Thus, we obtain:

$$g_{A \otimes A} = \frac{2\sqrt{2}}{[K_1 K_2]^{\frac{1}{4}}}.\tag{G.30}$$

Now consider coupled chains. The low energy Hamiltonian is:

$$H_b = 2i\gamma'_{-1}\Gamma_1 \cos\{\sqrt{\pi}r^{-1}[\cos\alpha\phi_\sigma(0) + \sin\alpha\phi_\rho(0)]\} \\ + 2i\gamma'_1\Gamma_2 \cos\{\sqrt{\pi}r[-\sin\alpha\phi_\sigma(0) + \cos\alpha\phi_\rho(0)]\}. \quad (\text{G.31})$$

Following the same logic as in Appendix G.2, the mode expansions are:

$$\cos\alpha\phi_\sigma(x) + \sin\alpha\phi_\rho(x) = r\sqrt{\pi}\frac{m_1x}{l} + \dots \\ -\sin\alpha\phi_\sigma(x) + \cos\alpha\phi_\rho(x) = r^{-1}\sqrt{\pi}\frac{m_2x}{l} + \dots \quad (\text{G.32})$$

Here m_1 and m_2 are arbitrary integers. Solving:

$$\phi_\sigma(x) = \sqrt{\pi}\frac{x}{l}(r\cos\alpha m_1 - \sin\alpha m_2/r) + \dots \\ \phi_\rho(x) = \sqrt{\pi}\frac{x}{l}(r\sin\alpha m_1 + \cos\alpha m_2/r) + \dots \quad (\text{G.33})$$

The corresponding terms in the energy are:

$$E = \frac{\pi}{2l}[u_\sigma K_\sigma(r\cos\alpha m_1 - \sin\alpha m_2/r)^2 + u_\rho K_\rho(r\sin\alpha m_1 + \cos\alpha m_2/r)^2] + \dots \quad (\text{G.34})$$

The corresponding factor in the partition function is:

$$Z \propto \int dm_1 dm_2 \exp\left\{-\frac{\pi}{2lT}\left[u_\sigma K_\sigma(r\cos\alpha m_1 - \sin\alpha m_2/r)^2 \right. \right. \\ \left. \left. + u_\rho K_\rho(r\sin\alpha m_1 + \cos\alpha m_2/r)^2\right]\right\} \\ = \frac{2lT}{\sqrt{u_\sigma u_\rho K_\sigma K_\rho}}. \quad (\text{G.35})$$

(As in Appendix G.1 the above integrals are easily done using the transformation $\vec{m}' = M^T \vec{m}$.) This determines:

$$g_{A\otimes A} = \frac{2\sqrt{2}}{[K_\rho K_\sigma]^{\frac{1}{4}}}. \quad (\text{G.36})$$

Now consider the implications of the g -theorem. From Eq. (G.36) and Eq. (G.20), we see that

$$g_{A\otimes A}/g_{N\otimes N} = \sqrt{\frac{2}{K_\rho K_\sigma}} \quad (\text{G.37})$$

This is larger than 1 for the range of Luttinger parameters likely to be of physical relevance, $K_\rho, K_\sigma < 1$. This implies that an RG flow from the $N \otimes N$ fixed point to the $A \otimes A$ fixed point is impossible, providing further evidence for the instability of the $A \otimes A$ fixed point. It can also be checked that quite generally $g_{A\otimes A} > g_{A\otimes N}$. For instance, in the case of decoupled channels, using Eqs. (G.25) and (G.30),

$$g_{A\otimes A}/g_{A\otimes N} = 2\sqrt{\frac{1}{K_2}} \quad (\text{G.38})$$

which is larger than 1 for the physically relevant range, $K_2 < 1$. In the next sub-section, we calculate g at the non-trivial critical point, using the ϵ -expansion. Since, for small ϵ this critical point is close to the unstable $N \otimes N$ point, we obtain a value of g_{NTCP} which is only slightly less than $g_{N\otimes N}$. This implies that $g_{A\otimes A} > g_{\text{NTCP}}$, so that the flow from the unstable $A \otimes A$ point to the non-trivial critical point respects the g -theorem.

Appendix G.4. Non-trivial critical point

In general, the value of g at the NTCP cannot be calculated analytically. It corresponds to a non-trivial universal property of the critical point, like its conductance, considered in Sec. III. Here we calculate it in the ϵ -expansion, introduced in Sec. II and used in Sec. III to obtain the conductance. The method we use is similar to that introduced in [34] with one important difference. In [34] a barely relevant ($0 < \epsilon \ll 1$) boundary perturbation was considered that had a cubic term in its β -function. An expression for g was obtained, $\propto \epsilon^3$, in terms of the coefficient of the cubic term. For the models considered here the cubic term in the β -function vanishes and it is necessary to analyse the quartic term. We find it convenient to develop a perturbative expansion for the impurity entropy, $\ln g$, rather than g itself:

$$S_{\text{imp}} \equiv \ln g = \ln g_{N \otimes N} - a \cdot \epsilon^2 \quad (\text{G.39})$$

where $g_{N \otimes N}$ is given in Eq. (G.20) and a is a number of order one which we will calculate. Of course, to second order in ϵ ,

$$g = g_{N \otimes N} [1 - a \cdot \epsilon^2]. \quad (\text{G.40})$$

In principle, the method is straightforward; we simply expand the log of the partition function in powers of the t_i and eventually evaluate the t_i at their critical values. What makes the calculation a bit tricky is that, in addition to corrections to the impurity entropy, we will also obtain non-universal corrections, e_1 , to the ground state energy:

$$\delta \ln Z = -e_1 \beta + \delta S_{\text{imp}}. \quad (\text{G.41})$$

These are distinguished by their dependence on the inverse temperature, β . e_1 is temperature independent. δS_{imp} has a weak temperature dependence $\propto \beta^{2\epsilon}$, associated with the RG flow of $t(\beta)$. To simplify the calculation, we first consider the symmetric case $\epsilon_1 = \epsilon_2$, along the separatrix, $t_1 = t_2 = t$.

We begin by expanding $\ln Z$ to second order in t :

$$\ln Z \approx \ln Z_0 + \frac{1}{2!} \int d\tau_1 d\tau_2 \mathcal{T} < H_b(\tau_1) H_b(\tau_2) >. \quad (\text{G.42})$$

At zero temperature, summing over both channels, we have:

$$\mathcal{T} < H_b(\tau_1) H_b(\tau_2) > = 4\tau_0^{-2\epsilon} t^2 \frac{1}{|\tau_{12}|^{2(1-\epsilon)}}. \quad (\text{G.43})$$

At finite temperature we make the replacement:

$$\tau_{12} \rightarrow (\beta/\pi) \sin(\pi\tau_{12}/\beta) \quad (\text{G.44})$$

which follows from a conformal transformation. Assuming $\tau_0 \ll \beta$, this gives:

$$\delta \ln Z \approx 4t^2 \tau_0^{-2\epsilon} \left(\frac{\pi}{\beta} \right)^{2(1-\epsilon)} \beta \int_{\tau_0}^{\beta/2} \frac{d\tau}{\sin^{2(1-\epsilon)}(\pi\tau/\beta)}. \quad (\text{G.45})$$

Changing variables to

$$u \equiv \tan(\pi\tau/\beta) \quad (\text{G.46})$$

this becomes:

$$\delta \ln Z \approx 4t^2 \pi \left(\frac{\beta}{\pi \tau_0} \right)^{2\epsilon} \int_{u_0}^{\infty} \frac{du}{(1+u^2)^\epsilon u^{2(1-\epsilon)}}. \quad (\text{G.47})$$

Here, the ultra-violet cut-off has become:

$$u_0 \equiv \pi \tau_0 / \beta \quad (\text{G.48})$$

for $\tau_0 \ll \beta$. In order to separate the ground state energy correction from the entropy correction, it is convenient to integrate by parts:

$$\delta \ln Z \approx -4t^2 \pi \left(\frac{\beta}{\pi \tau_0} \right)^{2\epsilon} \frac{1}{1-2\epsilon} \left[\frac{u_0^{2\epsilon-1}}{(1+u_0^2)^\epsilon} + 2\epsilon \int_{u_0}^{\infty} du \frac{u^{2\epsilon}}{(1+u^2)^{1+\epsilon}} \right]. \quad (\text{G.49})$$

The remaining integral is finite at $u_0 \rightarrow 0$. Since it already has a prefactor of ϵ we may evaluate it at $\epsilon = 0$, giving a simple integral. Thus, to lowest order in ϵ :

$$\delta \ln Z \approx -4t^2 \pi \left[\frac{\beta}{\pi \tau_0} + \epsilon \pi \left(\frac{\beta}{\tau_0} \right)^{2\epsilon} \right]. \quad (\text{G.50})$$

We have succeeded in separating this into a non-universal correction to the ground state energy, $e_1 = 4t^2 \pi / \tau_0$, of no interest, together with a correction to the impurity entropy:

$$\delta S_{\text{imp}} = -4t^2 \pi^2 \epsilon \left(\frac{\beta}{\tau_0} \right)^{2\epsilon}. \quad (\text{G.51})$$

We recognize:

$$t \left(\frac{\beta}{\tau_0} \right)^\epsilon = t(\beta), \quad (\text{G.52})$$

the renormalized coupling constant at scale β . To order t^2 only the lowest order renormalization of $t(\beta)$ appears but we expect that higher order terms will continue to give an expression for $\delta S_{\text{imp}}(\beta)$ which can be expressed in terms of the renormalized coupling constant $t(\beta)$ only. (This was shown explicitly in [34].) Thus, we write:

$$\delta S_{\text{imp}}(\beta) = -4\pi^2 \epsilon t(\beta)^2 + \dots \quad (\text{G.53})$$

where the \dots represents higher orders in the expansion in $t(\beta)$. Thus, in this approximation, the correction to the zero temperature impurity entropy is obtained by setting:

$$t(\beta) \rightarrow t_c = \sqrt{\epsilon / \mathcal{F}(\nu)}. \quad (\text{G.54})$$

(t_c was calculated in Sec. II.) Thus:

$$\delta S_{\text{imp}} = -\frac{4\pi^2 \epsilon^2}{\mathcal{F}(\nu)}. \quad (\text{G.55})$$

It is important to note that the impurity entropy *decreases* under renormalization, as required by the g-theorem.

Note that the correction to S_{imp} obtained so far, Eq. (G.51), is second order in t and contains an explicit factor of ϵ , making it $O(\epsilon^2)$. We must now go to fourth order in t looking for a term in δS_{imp} of order $\epsilon^0 t^4$ which is also $O(\epsilon^2)$. We will now show that

no such term exists and therefore Eq. (G.55) contains the entire correction to S_{imp} of $O(\epsilon^2)$. We begin with:

$$\delta \ln Z = \frac{1}{4!} \prod_{i=1}^4 \int' d\tau_i \mathcal{T} < H_b(\tau_1) H_b(\tau_2) H_b(\tau_3) H_b(\tau_4) > - \frac{1}{8} \left[\int' d\tau_1 d\tau_2 \mathcal{T} < H_b(\tau_1) H_b(\tau_2) > \right]^2. \quad (\text{G.56})$$

(Because we are calculating $\delta \ln Z$ rather than δZ itself, we subtract off the second order iteration of the term of $O(t^2)$ calculated above. This leads to very convenient cancellations. The ' on the integral signs signifies that we apply our ultra-violet cut-off, $|\tau_{ij}| > \tau_0$.) The fourth order matrix element is readily evaluated following the methods of Appendix B. There are two distinct contributions, $\propto t_j^4$ (with equal contributions for $j = 1$ or 2), and $\propto t_1^2 t_2^2$. We first consider the t_j^4 term. The needed fermionic factors are simply:

$$\mathcal{T} < \gamma(\tau_1) \gamma(\tau_2) \gamma(\tau_3) \gamma(\tau_4) > = \mathcal{T} < \Gamma_1(\tau_1) \Gamma_1(\tau_2) \Gamma_1(\tau_3) \Gamma_1(\tau_4) > = \epsilon(\tau_1, \tau_2, \tau_3, \tau_4) \quad (\text{G.57})$$

and square to one. Thus, at zero temperature we have:

$$\delta \ln Z = \tau_0^{-4\epsilon} \frac{t^4}{6} \prod_{i=1}^4 \int' d\tau_i \left[\left| \frac{\tau_{12}\tau_{34}}{\tau_{13}\tau_{14}\tau_{23}\tau_{24}} \right|^{2(1-\epsilon)} + \left| \frac{\tau_{13}\tau_{24}}{\tau_{12}\tau_{14}\tau_{23}\tau_{34}} \right|^{2(1-\epsilon)} + \left| \frac{\tau_{14}\tau_{23}}{\tau_{12}\tau_{13}\tau_{24}\tau_{34}} \right|^{2(1-\epsilon)} - 2 \left| \frac{1}{\tau_{12}\tau_{34}} \right|^{2(1-\epsilon)} - 2 \left| \frac{1}{\tau_{13}\tau_{24}} \right|^{2(1-\epsilon)} - 2 \left| \frac{1}{\tau_{14}\tau_{23}} \right|^{2(1-\epsilon)} \right]. \quad (\text{G.58})$$

As for the $O(t^2)$ term calculated above, we actually do the calculation at a low but finite temperature, β^{-1} , resulting in the substitution: $\tau_i \rightarrow (\beta/\pi) \sin(\pi\tau_i/\beta)$. It is convenient to use time-translation invariance to do the integral over τ_1 , giving a factor of β . We then change variables to:

$$\begin{aligned} u &= \tan(\pi\tau_2/\beta) \\ v &= \tan(\pi\tau_3/\beta) \\ w &= \tan(\pi\tau_4/\beta). \end{aligned} \quad (\text{G.59})$$

After a little algebra, the integral then becomes:

$$\delta \ln Z = \frac{\pi t^4}{6} \left(\frac{\beta}{\pi\tau_0} \right)^{4\epsilon} \int' \frac{du dv dw}{(1+u^2)^\epsilon (1+v^2)^\epsilon (1+w^2)^\epsilon} \left[\left| \frac{u(v-w)}{vw(u-v)(u-w)} \right|^{2(1-\epsilon)} + \left| \frac{v(u-w)}{uw(v-u)(v-w)} \right|^{2(1-\epsilon)} + \left| \frac{w(u-v)}{uv(w-u)(w-v)} \right|^{2(1-\epsilon)} - 2 \left| \frac{1}{u(v-w)} \right|^{2(1-\epsilon)} - 2 \left| \frac{1}{v(u-w)} \right|^{2(1-\epsilon)} - 2 \left| \frac{1}{w(u-v)} \right|^{2(1-\epsilon)} \right]. \quad (\text{G.60})$$

The ' on the integral sign now indicates that the u , v and w integrals run from $-\infty$ to ∞ , subject to the ultra-violet cut-off $|u|, |v|, |w|, |u-v|, |u-w|, |v-w| > u_0 \equiv \pi\tau_0/\beta$. Once again, we must disentangle terms in $\delta \ln Z \propto \beta/\tau_0$ which correspond to non-universal ground state energy corrections from terms $\propto t^4(\beta/\tau_0)^4 \propto t(\beta)^4$, corresponding to corrections to the impurity entropy. Note that the integrand in Eq. (G.60) diverges as

$u^{-4(1-\epsilon)}$ when u, v and w all go to zero proportional to each other. Since the integral is 3-dimensional, this implies $(\beta/\tau_0)^{1-4\epsilon}$ behavior, which when combined with the prefactor gives β/τ_0 , corresponding to a ground state energy term. In order to separate this ground state energy correction from the impurity entropy term, it is convenient to first change variables to $v' \equiv v/u$, $w' \equiv w/u$, then integrate by parts with respect to u . The u integral is now:

$$\begin{aligned} I(v', w') &\equiv \int_{u_0}^{\infty} du u^{4\epsilon-2} \left\{ \frac{1}{(1+u^2)[1+(uv')^2][1+(uw')^2]} \right\}^{\epsilon} \\ &= \frac{u_0^{4\epsilon-1}}{1-4\epsilon} \left\{ \frac{1}{(1+u_0^2)[1+(u_0v')^2][1+(u_0w')^2]} \right\}^{\epsilon} \\ &\quad - \frac{2\epsilon}{1-4\epsilon} \int_{u_0}^{\infty} du u^{4\epsilon-1} \left\{ \frac{1}{(1+u^2)[1+(uv')^2][1+(uw')^2]} \right\}^{\epsilon} \\ &\quad \left[\frac{u^2}{1+u^2} + \frac{(uv')^2}{1+(uv')^2} + \frac{(uw')^2}{1+(uw')^2} \right]. \end{aligned} \quad (\text{G.61})$$

Inserting the first term in Eq. (G.61) back into Eq. (G.60) gives a term in $\delta \ln Z \propto \beta/\tau_0$ corresponding to a ground state energy correction, while the second term in Eq. (G.61) gives a correction to S_{imp} which can be seen to be $\propto t^4 \epsilon \propto \epsilon^3$ and therefore negligible to the order we are working. To see this, we can set some unessential factor of $\epsilon \rightarrow 0$ in Eq. (G.61). Then the first term in Eq. (G.61) gives:

$$\begin{aligned} \delta \ln Z &= \frac{\pi t^4}{3} \frac{\beta}{\pi \tau_0} \int' dv' dw' \left[\left(\frac{v' - w'}{v'w'(1-v')(1-w')} \right)^2 + \left(\frac{v'(1-w')}{w'(1-v')(w'-v')} \right)^2 \right. \\ &\quad \left. + \left(\frac{w'(1-v')}{v'(1-w')(w'-v')} \right)^2 \right. \\ &\quad \left. - 2 \left(\frac{1}{v' - w'} \right)^2 - 2 \left(\frac{1}{v'(1-w')} \right)^2 - 2 \left(\frac{1}{w'(1-v')} \right)^2 \right]. \end{aligned} \quad (\text{G.62})$$

This integral can be seen to be ultraviolet finite when the cut-off goes to zero, due to cancellations between the six terms. For instance, the singular part of the integrand when $v' \rightarrow 0$ is

$$I \rightarrow \left(\frac{1}{v'(1-w')} \right)^2 \left[\left(\frac{1-v'/w'}{1-v'} \right)^2 + \left(\frac{1-v'}{1-v'/w'} \right)^2 - 2 \right] \rightarrow \frac{4}{(1-w')^2} \left[\frac{1}{(w')^2} + 1 \right]. \quad (\text{G.63})$$

The sum of the three terms inside the brackets scale as $(v')^2$ as $v' \rightarrow 0$, leaving a finite limiting value for the integrand. The integral in Eq. (G.62) can also be seen to converge at $|v'|, |w'| \rightarrow \infty$. (At large v', w' the second, third and fourth terms almost cancel each other.) Therefore Eq. (G.62) gives a term in $\delta \ln Z$ which is β/τ_0 times a finite number, corresponding to a ground state energy correction. Of greater interest is the result of inserting the second term in Eq. (G.61) back into Eq. (G.60). This gives the correction to S_{imp} . Converting back to the original v and w integration variables for convenience, and setting inessential factors of ϵ to zero, this gives:

$$\delta \ln Z = - \frac{2\pi t^4}{6} \left(\frac{\beta}{\pi \tau_0} \right)^{4\epsilon} \epsilon \int' du dv dw \left[\frac{u^2}{1+u^2} + \frac{v^2}{1+v^2} + \frac{w^2}{1+w^2} \right]$$

$$\left\{ \left(\frac{u(v-w)}{vw(u-v)(u-w)} \right)^2 + \left(\frac{v(u-w)}{uw(u-v)(v-w)} \right)^2 + \left(\frac{w(u-v)}{vu(u-w)(v-w)} \right)^2 - 2 \left(\frac{1}{u(v-w)} \right)^2 - 2 \left(\frac{1}{v(u-w)} \right)^2 - 2 \left(\frac{1}{w(v-u)} \right)^2 \right\} \quad (\text{G.64})$$

Again, Taylor expanding the expression in curly brackets around the singular points, $u \rightarrow 0$, $u \rightarrow v$ et cetera shows that this integral is finite when the ultra-violet cut-off is taken to zero. It also converges at $|u|, |v|, |w| \rightarrow \infty$. (This is fairly obvious since the integrand of this 3-dimensional integral scales as $1/u^4$ when $|u|, |v|$ and $|w|$ all go to ∞ proportional to each other.) Therefore it gives a correction $\delta \ln Z \propto \epsilon t^4 (\beta/\tau_0)^{4\epsilon} = \epsilon t (\beta)^4$. In the zero temperature limit, we can replace the running coupling constant, $t(\beta)$ by its fixed point value t_c , giving a correction $\delta \ln Z \propto \epsilon^3$, negligible compared to Eq. (G.55).

Finally, we consider the term in $\delta \ln Z \propto t_1^2 t_2^2$, showing that it is again $\propto \epsilon t_c^4 \propto \epsilon^3$. The fermion factors now give:

$$\begin{aligned} \mathcal{T} < \Gamma_1(\tau_1) \Gamma_1(\tau_2) \Gamma_2(\tau_3) \Gamma_2(\tau_4) > \mathcal{T} < \gamma(\tau_1) \gamma(\tau_2) \gamma(\tau_3) \gamma(\tau_4) > \\ = \epsilon(\tau_1 - \tau_2) \epsilon(\tau_3 - \tau_4) \epsilon(\tau_1, \tau_2, \tau_3, \tau_4) = \epsilon(\tau_1 - \tau_3) \epsilon(\tau_1 - \tau_4) \epsilon(\tau_2 - \tau_3) \epsilon(\tau_2 - \tau_4). \end{aligned} \quad (\text{G.65})$$

$\epsilon(\tau)$ and $\epsilon(\tau_1, \tau_2, \tau_3, \tau_4)$ are the anti-symmetric step functions defined in Appendix B, not to be confused with $\epsilon = d_b - 1$, the scaling dimension. The bosonic factor is:

$$\begin{aligned} 16 < \cos[\sqrt{\pi} \phi_1(\tau_1)] \cos[\sqrt{\pi} \phi_1(\tau_2)] \cos[\sqrt{\pi} \phi_2(\tau_3)] \cos[\sqrt{\pi} \phi_1(\tau_4)] > \\ = 2 \left(\frac{1}{(\tau_1 - \tau_2)(\tau_3 - \tau_4)} \right)^{2(1-\epsilon)} \left[\left| \frac{(\tau_1 - \tau_3)(\tau_2 - \tau_4)}{(\tau_1 - \tau_4)(\tau_2 - \tau_3)} \right|^\nu + \left| \frac{(\tau_1 - \tau_4)(\tau_2 - \tau_3)}{(\tau_1 - \tau_3)(\tau_2 - \tau_4)} \right|^\nu \right] \end{aligned} \quad (\text{G.66})$$

where ν is defined in Eq. (28). Thus, at zero temperature:

$$\begin{aligned} \delta \ln Z = t^4 \prod_{i=1}^4 \int' d\tau_i \left(\frac{1}{(\tau_1 - \tau_2)(\tau_3 - \tau_4)} \right)^{2(1-\epsilon)} \left\{ -2 \right. \\ \left. + \left\{ \left[\left| \frac{(\tau_1 - \tau_3)(\tau_2 - \tau_4)}{(\tau_1 - \tau_4)(\tau_2 - \tau_3)} \right|^\nu + \left| \frac{(\tau_1 - \tau_4)(\tau_2 - \tau_3)}{(\tau_1 - \tau_3)(\tau_2 - \tau_4)} \right|^\nu \right] \epsilon(\tau_1 - \tau_3) \epsilon(\tau_1 - \tau_4) \epsilon(\tau_2 - \tau_3) \epsilon(\tau_2 - \tau_4) \right\} \right\} \end{aligned} \quad (\text{G.67})$$

Passing to finite temperature via Eq. (G.44), integrating over τ_1 , and then changing variables as in Eq. (G.59) turns this into:

$$\begin{aligned} \delta \ln Z = \pi t^4 \left(\frac{\beta}{\pi \tau_0} \right)^{4\epsilon} \int' \frac{dudvdw}{(1+u^2)^\epsilon (1+v^2)^\epsilon (1+w^2)^\epsilon} \left| \frac{1}{u(v-w)} \right|^{2(1-\epsilon)} \\ \cdot \left\{ \left[\left| \frac{v(u-w)}{w(u-v)} \right|^\nu + \left| \frac{w(u-v)}{v(u-w)} \right|^\nu \right] \epsilon(v) \epsilon(w) \epsilon(u-v) \epsilon(u-w) \right] - 2 \right\}. \end{aligned} \quad (\text{G.68})$$

To separate the ground state energy correction from the impurity entropy correction, we again rescale and integrate by parts, as above. The needed u -integral is the same

one as in Eq. (G.61). The first term in Eq. (G.61) then gives, after dropping inessential factors of ϵ :

$$\begin{aligned} \delta \ln Z &= 2\pi t^4 \frac{\beta}{\pi \tau_0} \int' \frac{dv' dw'}{(v' - w')^2} \\ &\times \left\{ \left[\left| \frac{v'(1-w')}{w'(1-v')} \right|^\nu + \left| \frac{w'(1-v')}{v'(1-w')} \right|^\nu \right] \epsilon(v') \epsilon(w') \epsilon(1-v') \epsilon(1-w') - 2 \right\}. \end{aligned} \quad (\text{G.69})$$

Taylor expanding the quantity in curly brackets around the point $v' = w'$ it can be seen that it is $O[(v' - w')^2]$, and so there is no ultra-violet divergence in that limit. For the range of Luttinger parameters and anisotropy parameter α that we are considering, $0 < \nu \leq 1$, so there is no ultraviolet divergence at $v', w' \rightarrow 0, 1$. To see this in the limiting $SU(2)$ invariant case, $\nu = 1$, we may use:

$$\begin{aligned} &\left[\left| \frac{v'(1-w')}{w'(1-v')} \right| + \left| \frac{w'(1-v')}{v'(1-w')} \right| \right] \epsilon(v') \epsilon(w') \epsilon(1-v') \epsilon(1-w') \\ &= \frac{(v')^2(1-w')^2 + (w')^2(1-v')^2}{v'w'(1-v')(1-w')}. \end{aligned} \quad (\text{G.70})$$

Then integrating symmetrically around the singularities at $v', w' = 0, 1$ gives a finite result. Thus we take the ultraviolet cut off to zero in evaluating this integral. The integral can also be seen to converge at $|v'|, |w'| \rightarrow \infty$ and thus Eq. (G.70) gives β/τ_0 times a finite number, corresponding to a ground state energy correction. The second term in Eq. (G.61), after taking inessential factors of $\epsilon \rightarrow 0$, gives:

$$\begin{aligned} \delta \ln Z &= 2\pi t^4 \left(\frac{\beta}{\pi \tau_0} \right)^{4\epsilon} \epsilon \int' dudv dw \left(\frac{1}{u(v-w)} \right)^2 \left[\frac{u^2}{1+u^2} + \frac{v^2}{1+v^2} + \frac{w^2}{1+w^2} \right] \\ &\cdot \left\{ \left[\left| \frac{v(u-w)}{w(u-v)} \right|^\nu + \left| \frac{w(u-v)}{v(u-w)} \right|^\nu \right] \epsilon(v) \epsilon(w) \epsilon(u-v) \epsilon(u-w) - 2 \right\} \end{aligned} \quad (\text{G.71})$$

Again by Taylor expanding the quantity in curly brackets we can see that there is no divergence at $v \rightarrow w$ or $u \rightarrow 0$. Nor are there any divergences at $v, w \rightarrow 0, u$ for $0 < \nu \leq 1$. The integral can also be seen to converge at $|u|, |v|, |w| \rightarrow \infty$. Thus we obtain $t(\beta)^4 \epsilon$ times a finite constant. This again gives a correction to S_{imp} of $O(\epsilon^3)$, completing our proof that Eq. (G.55) gives the entire correction of $O(\epsilon^2)$.

In the above calculation, we assumed $\epsilon_1 = \epsilon_2$, for simplicity. But the quadratic term giving Eq. (G.55) just consisted of a sum of contributions from each channel, so it follows that in general:

$$\delta S_{\text{imp}} = -\frac{2\pi^2(\epsilon_1^2 + \epsilon_2^2)}{\mathcal{F}} + O(\epsilon^3) \quad (\text{G.72})$$

and g at the non-trivial critical point is given by:

$$g_{\text{NTCP}} \approx g_{N \otimes N} \left[1 - \frac{2\pi^2}{\mathcal{F}}(\epsilon_1^2 + \epsilon_2^2) \right] = 2(K_\sigma K_\rho)^{1/4} \left[1 - \frac{2\pi^2}{\mathcal{F}}(\epsilon_1^2 + \epsilon_2^2) \right] \quad (\text{G.73})$$

where the function $\mathcal{F}(\nu)$ is given by the integral in Eq. (B.41), plotted in Fig. (B1). [ν is given in terms of Luttinger parameters and anisotropy parameter α , in Eq. (28).]

References

- [1] V. Mourik, K. Zuo, S.M. Frolov, S.R. Plissard, E.P.A.M. Bakkers and L.P. Kowenhoven, *Science*, **336**, 1003 (2012).
- [2] R. M. Lutchyn, J. D. Sau, and S. Das Sarma, *Phys. Rev. Lett.* **105**, 077001 (2010).
- [3] Y. Oreg, G. Refael, and F. von Oppen, *Phys. Rev. Lett.* **105**, 177002 (2010).
- [4] K. T. Law, P. A. Lee, and T. K. Ng, *Phys. Rev. Lett.* **103**, 237001 (2009).
- [5] J. D. Sau, R. M. Lutchyn, S. Tewari, and S. Das Sarma, *Phys. Rev. Lett.* **104**, 040502 (2010).
- [6] J. Alicea, *Phys. Rev.* **B 81**, 125318 (2010).
- [7] M. Wimmer, A. R. Akhmerov, J. P. Dahlhaus, and C. W. J. Beenakker, *New J. Phys.* **13**, 053016 (2011).
- [8] A. Cook and M. Franz, *Phys. Rev.* **B84**, 201105 (2011).
- [9] J. Klinovaja and D. Loss, *Phys. Rev.* **B86**, 085408 (2012).
- [10] D. Sticlet, C. Bena, and P. Simon, *Phys. Rev. Lett.* **108**, 096802 (2012).
- [11] D. Chevallier, D. Sticlet, P. Simon, and C. Bena, *Phys. Rev.* **B85**, 235307 (2012).
- [12] B. Béri, N.R. Cooper, *Phys. Rev. Lett.* **109**, 156803 (2012).
- [13] L. Fidkowski, J. Alicea, N. H. Lindner, R. M. Lutchyn, and M. P. A. Fisher, *Phys. Rev.* **B 85**, 245121 (2012).
- [14] I. Affleck, J.-S. Caux and A. Zagoskin, *Phys. Rev.* **B62**, 1433 (2000).
- [15] J. Alicea, Y. Oreg, G. Refael, F. von Oppen and M.P.A. Fisher, *Nat. Phys.* **7**, 412 (2011).
- [16] D. Giuliano and I. Affleck, in preparation.
- [17] D. Giuliano and I. Affleck, *J. Stat. Mech.* P02034 (2013).
- [18] B. Béri, *Phys. Rev. Lett.* **110**, 216803 (2013).
- [19] A. H. Castro Neto, E. Novais, L. Borda, G. Zaránd, and I. Affleck, *Phys. Rev. Lett.* **91**, 096401 (2003).
- [20] E. Novais, A. H. Castro Neto, L. Borda, I. Affleck, and G. Zaránd, *Phys. Rev.* **B 72**, 014417 (2005).
- [21] E. Novais, F. Guinea, and A. H. Castro Neto, *Phys. Rev. Lett.* **94**, 170401 (2005).
- [22] C.G. Callan and D. Freed, *Nucl. Phys.* **B374**, 543 (1992).
- [23] G. Zaránd and E. Demler, *Phys. Rev.* **B66**, 024427 (2002).
- [24] S. M. Lukyanov, A. M. Tsvelik, and A. B. Zamolodchikov, *Nucl.Phys.* **B719**, 103 (2005).
- [25] C.L. Kane and M.P.A. Fisher, *Phys. Rev.* **B46**, 15233 (1992).
- [26] Eq. (3.12) of [25] appears to be missing a factor of $(e^2/h)\tau_c^{2n^2/g}$. We can ignore the powers of τ_c , or τ_0 in our notation, since we have effectively adsorbed them into our definition of the t_j as follows from Eq. (16). We included the factor of e^2/h in extracting the conductance from [25].
- [27] M. Oshikawa, C. Chamon and I. Affleck, *J.Stat.Mech.* 0602:P02008 (2006).
- [28] See, for example, the textbook: J.L. Cardy, *Scaling and Renormalization in Statistic Physics*, Cambridge University Press, 1996.
- [29] The third order term in the β -function of the Kondo model was calculated by a similar technique in I. Affleck and A.W.W. Ludwig, *Nucl. Phys.* **B360**, 641 (1991).
- [30] I. Affleck, *J. Phys. A: Math. Gen.* **31**, 2761 (1998).
- [31] J.R. Schrieffer and P.A. Wolff, *Phys. Rev.* **149**, 491492 (1966).
- [32] [13] gives this dimension at the $A \otimes N$ fixed point, in the symmetric case, $\alpha = \pi/4$, but seems to contain a “typo” about which operator it corresponds to.
- [33] I. Affleck and A.W.W. Ludwig, *Phys. Rev. Lett.* **67**, 161 (1991).
- [34] I. Affleck and A.W.W. Ludwig, *PRB* **48**, 7279 (1993).
- [35] D. Friedan and A. Konechny, *Phys. Rev. Lett.* **93**, 030402, (2004).
- [36] P. Calabrese, J. Cardy, *J. Stat. Mech.* 0406:P06002 (2004).
- [37] H.W.J. Blöte, J.L. Cardy and M.P. Nightingale, *Phys. Rev. Lett.* **56**, 742 (1986); I. Affleck, *ibid* **746** (1986).
- [38] This formula, for the case of a single channel and no superconductor, was derived by this method

in S. Eggert and I. Affleck, Phys. Rev. **B46**, 10866 (1992) but the square root was omitted from the final answer. It was rederived correctly by a different method in M. Oshikawa and I. Affleck, Nucl. Phys. **B495**, 533 (1997).